東　海　大　學

資訊工程研究所

碩士論文

指導教授：黃育仁 博士

以三維高解析血流都卜勒超音波影像特徵

進行乳癌前置化療分子亞型之評估

Molecular subtype evaluation for neo-adjuvant chemotherapy

of breast cancer: dependent on

3D high-definition flow power Doppler ultrasonic features

研究生：王雪綸

中　華　民　國　一　零　五　年　七　月

Molecular subtype evaluation for neo-adjuvant chemotherapy of breast cancer: dependent on 3D high-definition flow power Doppler ultrasonic features

Advisor

Prof. Yu-Len Huang

Submitted to the Department of Computer Science of

Tunghai University

in partial fulfillment of the requirements for the degree of

Master of Engineering

by

Hsueh-Lun Wang

July 2016

東海大學碩士學位論文考試審定書

東海大學資訊工程學系 研究所

研究生 王 雪 綸 所提之論文

以三維高解析血流都卜勒超音波影像特徵進行乳癌前置化療分子亞型之評估

經本委員會審查，符合碩士學位論文標準。

學位考試委員會

召 集 人 王經篤 簽章

委 員 張分易

黃育仁

黃育仁

指 導 教 授 ＿＿＿＿＿＿ 簽章

中華民國 105 年 7 月 5 日

摘要

對國人女性而言，乳癌的發生率逐年上升，近年來由於醫學研究的發展與進步，及早發現並接受治療能夠提高乳癌的治癒率，常見的檢查方式包含乳房超音波、乳房 X 光攝影及磁振造影等。乳房超音波檢查具有非放射性、非侵入性與成本較低的優點，再者台灣女性的乳房多屬緻密性質，這一特性於超音波檢查下較乳房 X 光攝影更易於偵測到腫瘤。本研究使用的高解析血流(high-definition flow, HDF)都卜勒超音波，是都卜勒超音波中能更有效地發現腫瘤位置並能提供血流方向及強度資訊的一項技術，更為適用於檢測乳房腫瘤。

血管增生現象為一與惡性腫瘤相關的重要因素，可應用於評估手術前新輔助化療之效果與乳癌分子亞型之間的關聯性。本研究利用一個自動提取腫瘤區域之血管中心線的方法，由血管中心線估計出 5 項血管量化指數、2 項腫瘤量化特徵，並且自都卜勒超音波影像中擷取 6 項乳癌腫瘤之形態學特徵，共計 13 項特徵進行研究。本論文採用 76 筆病患資料，針對前置化療第 0 期至第 3 期之各項特徵資料在各階段之間的差異值，對應由賀爾蒙受體為分類依據之五種乳癌分子亞型，以單變量變異數分析，觀察特徵與乳癌分子亞型之間的關聯性。

關鍵字：乳房腫瘤、乳房超音波、腫瘤血管、前置性化療、分子亞型

ABSTRACT

Breast cancer is the most common cancer affecting females. In recent years, due to the development of medical research, early detection and treatment can increase the cure rate of breast cancer. Breast ultrasound is not radioactive, non-invasive, and it could easier detect tumors than mammography. In this study, high-definition flow (HDF) Doppler ultrasound is performed to investigate blood flow and solid directional flow information in breast tumors.

Tumor vascularity, an important factor correlated with tumor malignancy, would be used to evaluate the effect of the neo-adjuvant chemotherapy prior to surgery and their correlation in the molecular subtypes of breast cancer. This study utilizes an automatic method to extract vascular centre-lines from the tumor area. The vascularity quantization is estimated from the vascular centre-lines, in addition, the morphology features are extracted from ultrasound images. This study includes 76 patients with breast cancer treated with neo-adjuvant chemotherapy. Finally, through one-way analysis of variance (ANOVA), observing the association between breast cancer molecular subtypes and each period of neo-adjuvant chemotherapy.

Keywords: breast tumor, breast ultrasound, tumor vascularity, neo-adjuvant chemotherapy, molecular subtype

TABLE OF CONTENTS

LIST OF TABLES

LIST OF FIGURES

CHAPTER 1

INTRODUCTION

Breast cancer is the most common cancer affecting females worldwide. In recent years, due to the development of medical research, early detection and treatment can increase the cure rate of breast cancer [1, 2]. Breast cancer develops from breast tissue that signs may include change in breast shape, dimpling of the skin, fluid coming from the nipple, or a red scaly patch of skin. There may be bone pain, swollen lymph nodes, shortness of breath, or yellow skin in those with distant spread of the disease. Generally, an exam of the body by self could checking signs of breast cancer [1, 3], such as lumps or anything else that seems unusually; otherwise, exam of the breast by a doctor or other professional person could getting more accurate clinical checking. The diagnosis of breast cancer is confirmed by taking a biopsy of the concerning lump [4]. Once the diagnosis was made, further imaging examinations were executed to determine treatment.

The common screening methods to obtain imaging of breast include mammogram, ultrasound and magnetic resonance imaging (MRI) [5]. Mammography is a specialized medical imaging that performs a low-dose x-ray system to see inside the breasts [6]. The advantage of mammography is that it could present more micro-calcifications of breast [7], the procedure is uncomplicated and not time-consuming. Several studies committed to predicting chemotherapy effect through mammography, such as tumor size of detected micro-calcifications [8], mammographic density [9] and texture features of mammogram [10]. However, even the mammogram is a noninvasively medical examination, the x-ray involves exposing a part of body to a small dose of ionizing radiation to produce pictures. Besides, patient must oppress breast during procedure of mammography that for some females will feel pain and fear to do inspection. For

oriental females, breast composition is denser than western women, lead to determine become difficult because the imaging of mammogram would present more white color area [11]. MRI is the most advanced technique of breast imaging that is a noninvasively and non-radiative medical examination [12]. It has an excellent resolution for soft tissues, and MRI can freely select the desired cross-section by adjusting the magnetic field. However, patients need to take a long time stationary to obtain MRI image that bring about patient uncomfortable. However, in some cases the performance of MRI might not better than computerized tomography (CT) [13], but the spending is expensive than CT or other diagnosis tools. Breast ultrasound is an appropriate imaging method for eastern females because that could clearly distinguish between solid substances or liquid parts. Ultrasound involves the use of small probe and ultrasound gel placed directly on the skin; patients would not feel pain or hurt in the examination [14]. Doppler ultrasound [15, 16] is a special ultrasound technique that allows the physician to see and evaluate blood flow through arteries and veins in the organs.

Recent years, more and more studies aim to early pre-diagnosis of breast cancer [17]. The association between dangerous factors of breast cancer and effect of breast cancer chemotherapy or neo-adjuvant chemotherapy [18] was gradually being taken seriously. Common breast cancer risk factors such as family history of breast cancer, age, pregnancy, obesity, hormone replacement therapy, oral contraceptives, smoking and alcohol were discussed in past years. On the other hand, many studies tried to found the connection between efficacy of treatment and hormone markers or biomarkers. The molecular biomarkers that estrogen receptors (ER), progesterone receptors (PR), and human epidermal growth factor receptor 2 (HER2) were also regularly apply to pre-diagnosis [19]. Breast cancer could divide into several subtypes by the biomarkers and then doctors could decide treatment for different subtypes.

In this study, the 3D HDF Doppler ultrasound was performed to investigate blood flow and solid directional flow information in breast tumors [20]. To pre-diagnosis the effect of neo-adjuvant chemotherapy, 13 characteristics was extracted from breast cancer tumors including five vascular features, six morphological features and two tumor quantification features. In connection with molecular subtypes and tumor features, this study performed the one-way ANOVA as statistical analysis tool to observed the association with significance difference of each features [21]. Finally, this study found that some features might have association with neo-adjuvant chemotherapy.

CHATPER 2

MATERIALS

2.1 Patients and Data Acquisition

76 patients who received neo-adjuvant chemotherapy from July 2007 to October 2010 with consecutive T2 breast cancer (Tumor size > 2cm and ≦ 5cm) were included in this study. The diagnosis of breast cancer was made by core needle biopsy. The Neo-adjuvant chemotherapy included six to eight courses and three weeks per cycle. Patients received sonographic examination by three-dimensional (3D) power Doppler ultrasound with HDF function (Voluson 730, GE Medical System, Zipf, Austria) at every stage. The stage N0 was the sonographic examination before the chemotherapy.

2.2 Neo-adjuvant Chemotherapy Response

The clinical tumor response was classified as four evaluations of lesions described as followed [22]:

- Complete response (CR): All target lesions were disappeared and no new lesions relapses at least continue four weeks. Any pathological lymph nodes (whether target or non-target) must have reduction in short axis < 10 mm.
- Partial response (PR): At least a 30% decrease in the sum of the longest diameter of target lesions, taking as reference the baseline sum longest diameter.
- Stable disease (SD): Neither sufficient shrinkage to qualify for PR nor sufficient increase to qualify for PD, taking as reference the smallest sum diameters.
- Progressive disease (PD): At least a 20% increase in the sum of the longest diameter of target lesions, taking as reference the smallest sum longest diameter recorded since the treatment started or the appearance of one or more

new lesions. In addition to the relative increase of 20%, the sum must also demonstrate an absolute increase of at least 5 mm. (Note: the appearance of one or more new lesions is also considered progression).

Figure 2.1 shows that the ultrasound image of different neo-adjuvant chemotherapy responses using software GE Kretz 4D View (GE Kretztechnik, Zipf, Austria).

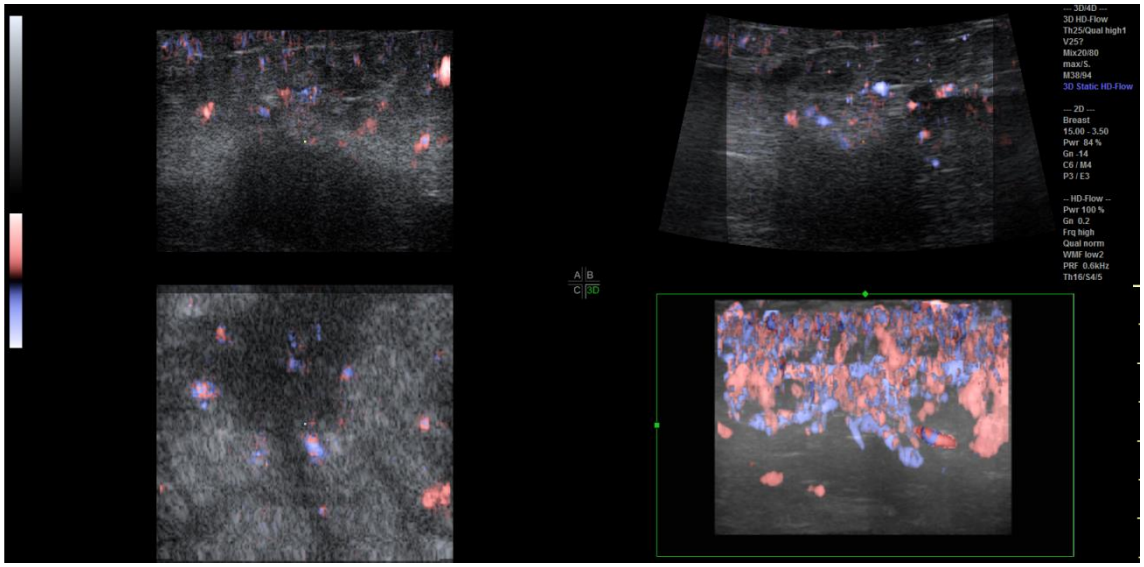

(a)

Figure 2.1: 3D HDF power Doppler ultrasound image of (a) CR patient (b) PR patient (c) SD patient (d) PD patient using software GE Kretz 4D View (Continued)

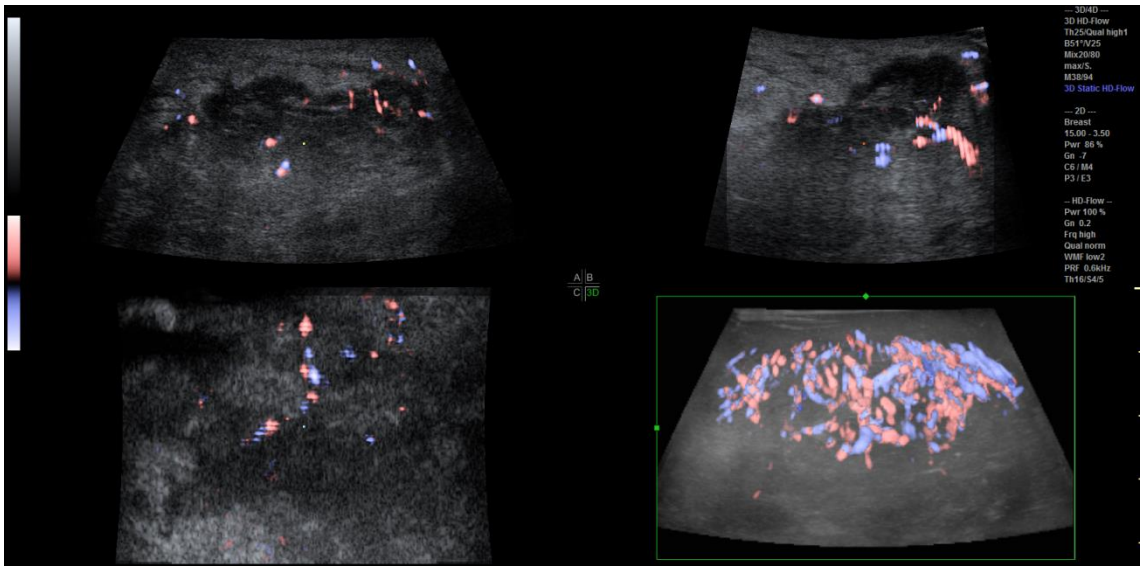

(b)

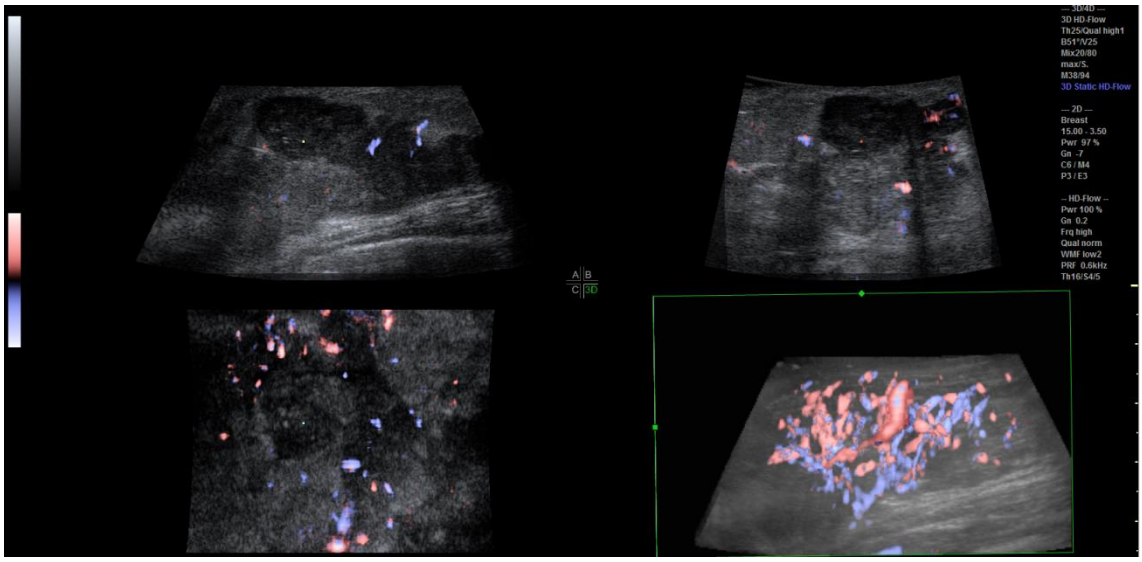

(c)

Figure 2.1: 3D HDF power Doppler ultrasound image of (a) CR patient (b) PR patient (c) SD patient (d) PD patient using software GE Kretz 4D View (Continued)

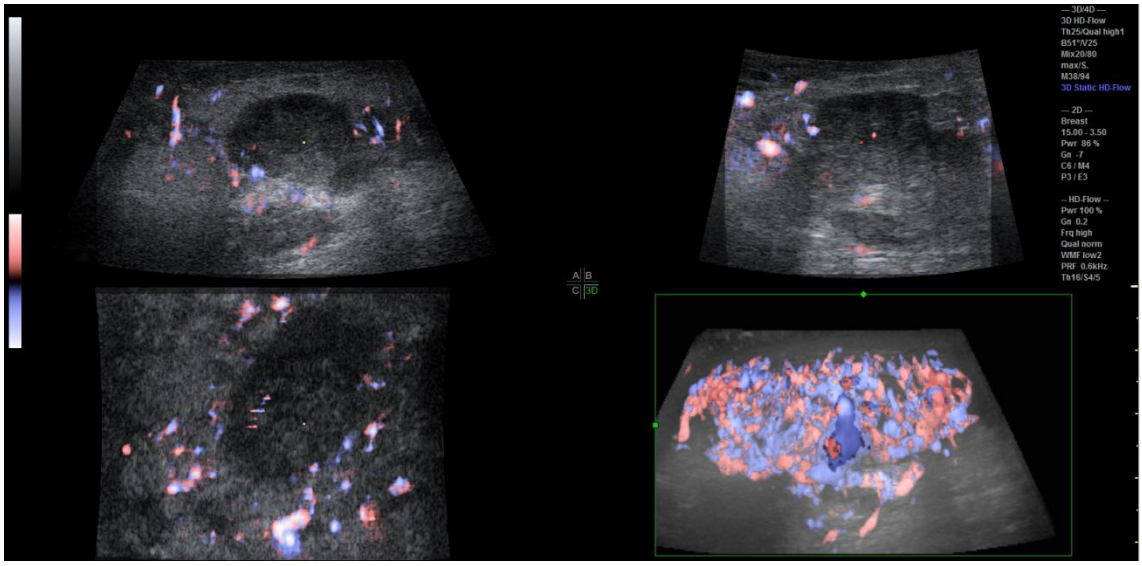

(d)

Figure 2.1: 3D HDF power Doppler ultrasound image of (a) CR patient (b) PR patient (c) SD patient (d) PD patient using software GE Kretz 4D View

Among the 76 cases, the ratio of CR, PR, SD and PD was 26.3%, 47.4%, 19.7% and 6.6%, respectively. Table 2.1 shows the case number of CR, PR, SD and PD.

Table 2.1: The case number of neo-adjuvant chemotherapy response

Neo-adjuvant chemotherapy response	Number of cases
CR	20 (26.3%)
PR	36 (47.4%)
SD	15 (19.7%)
PD	5 (6.6%)
Total cases	76

CR: complete response; PR: partial response; SD: stable disease; PD: progressive disease.

Usually, the patients were classified into two groups: the good responder, who was classified as CR or PR, and the poor responder, who was classified as SD or PD. The case number of good response and poor response is showed in Table 2.2.

Table 2.2: The case number of good response and poor response

Response	Number of cases
Good	56 (73.7%)
Poor	20 (26.3%)
Total cases	76

Furthermore, another classified way is the complete response, that was CR, and the no response means PR, SD, and PD. The case number of complete response and no response is showed in Table 2.3.

Table 2.3: The case number of complete response and no response

Response	Number of cases
Complete	20 (26.3%)
No	56 (73.7%)
Total cases	76

2.3 Molecular Subtypes

Prognostic factors of breast cancer become an important issue in recently. Receptors proteins could attach to certain substances in or on certain cells circulate in the blood. Normal breast cells and some breast cancer cells contain estrogen receptors, progesterone receptors and HER2 [19]. Estrogen receptors and progesterone receptors receive hormone signals informing the cell to grow. HER2 receptors control growth, division, and repair of breast cells. In this study, patients was classified into five molecular subtypes based on immunohistochemistry of breast cancer, including luminal A, luminal B1, luminal B2, HER2 overexpressing and triple negative (TN) [23]. Table 2.4 shows the expression of hormone receptors.

Table 2.4: The hormone receptors expression of molecular subtypes

Subtype	Estrogen receptors	Progesterone receptors	HER2
Luminal A	+	+ [a]	−
Luminal B1	+	+ [b]	−
	−	+	−
	+	−	−
Luminal B2	+	+	+
	−	+	+
	+	−	+
HER2 enriched	−	−	+
TN	−	−	−

TN: triple negative breast cancer; HER2: human epidermal growth factor receptor 2.

[a] The progesterone receptors at luminal A subtype is plus at least 20% of classification.

[b] The progesterone receptors at luminal B1 subtype is plus less than 20% of classification.

In the 76 patients, six cases were luminal A, 36 cases were luminal B1, 18 cases were luminal B2, ten cases were HER2 overexpressing and six cases were TN. Table 2.5 shows the case number of good response and complete response corresponds to molecular subtypes. In addition, the association between the case number of neo-adjuvant chemotherapy responses (CR, PR, SD and PD) and molecular subtypes are also showed at Table 2.5. Figure 2.2 shows the ultrasound images which are the example cases of each molecular subtype from the software GE Kretz 4D View.

Table 2.5: Neo-adjuvant response of patients

	Luminal A	Luminal B1	Luminal B2	HER2	TN	p-value
Cases	6 (8%)	36 (47%)	18 (24%)	10 (13%)	6 (8%)	
Good Response	4	25	14	10	3	0.209
Complete Response	0	4	6	7	3	< 0.001
CR	0	4	6	7	3	< 0.001
PR	4	21	8	3	0	0.051
SD	0	10	4	0	1	0.247
PD	2	1	0	0	2	0.001

TN: triple negative breast cancer; CR: complete response; PR: partial response; SD: stable disease; PD: progressive disease.

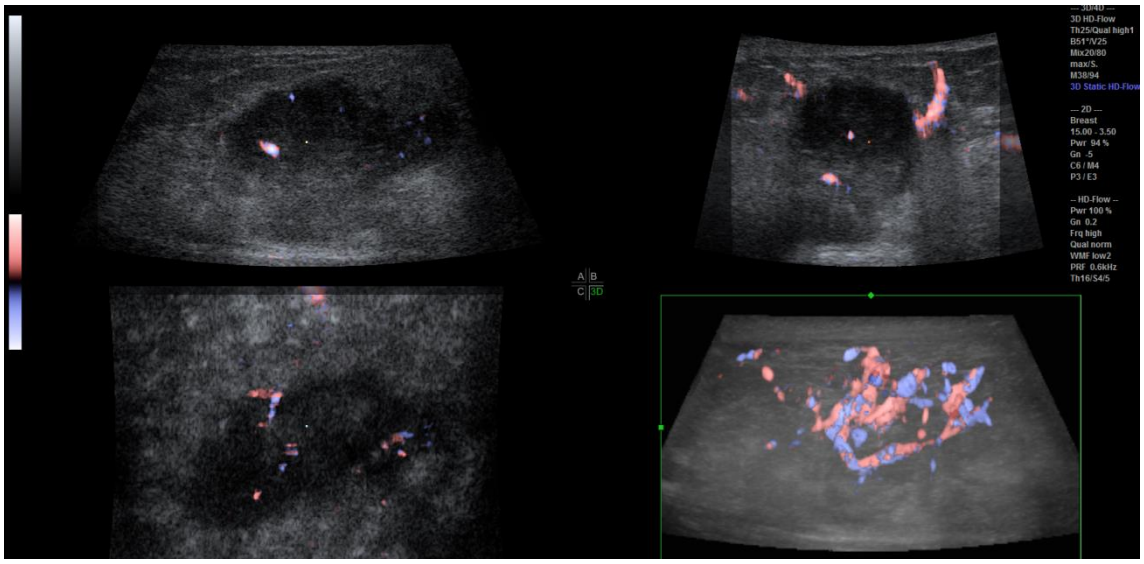

(a)

Figure 2.2: 3D HDF power Doppler ultrasound image of (a) luminal A (b) luminal B1 (c) luminal B2 (d) HER2 overexpressing (e) TN patient from the software GE Kretz 4D View (Continued)

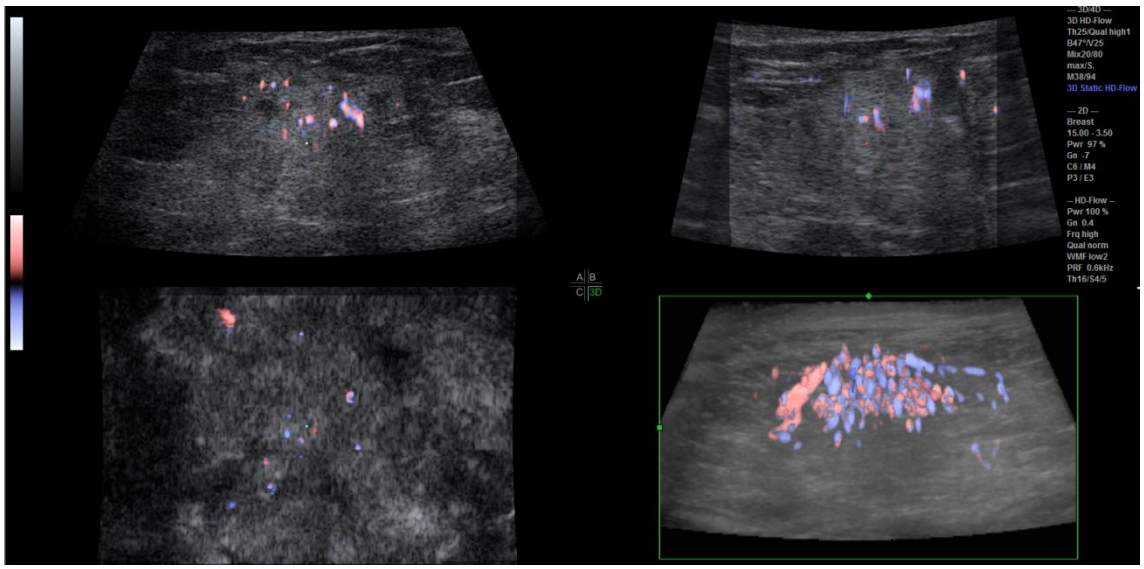

(b)

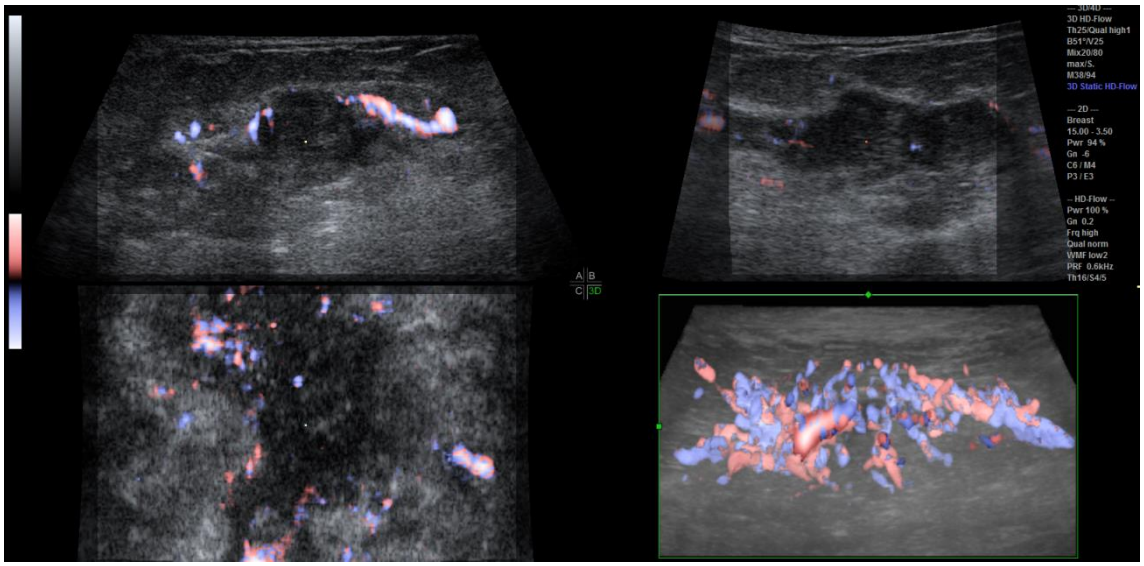

(c)

Figure 2.2: 3D HDF power Doppler ultrasound image of (a) luminal A (b) luminal B1 (c) luminal B2 (d) HER2 overexpressing (e) TN patient from the software GE Kretz 4D View (Continued)

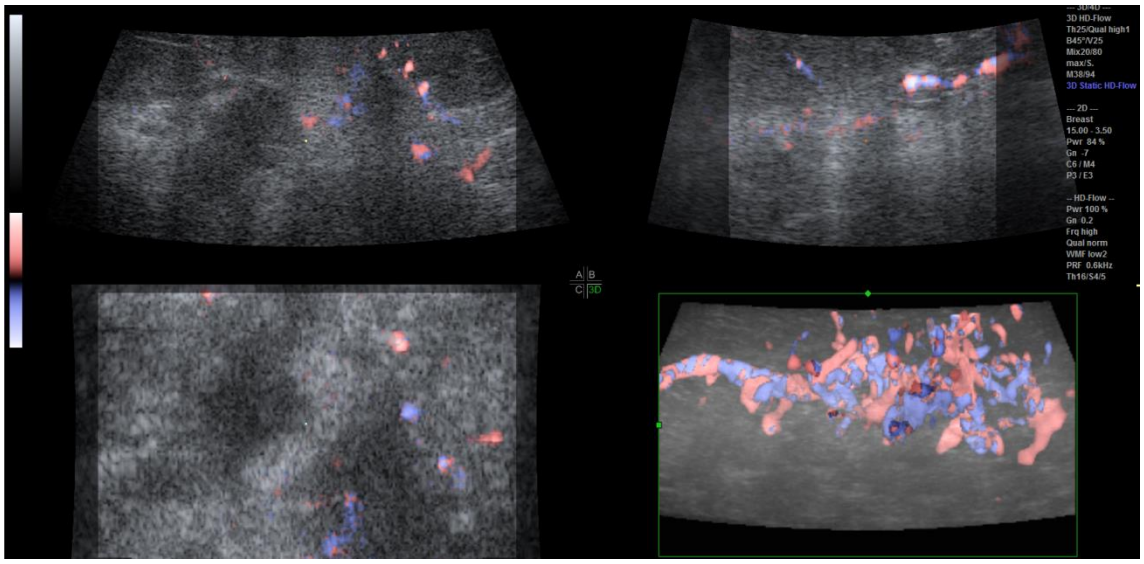

(d)

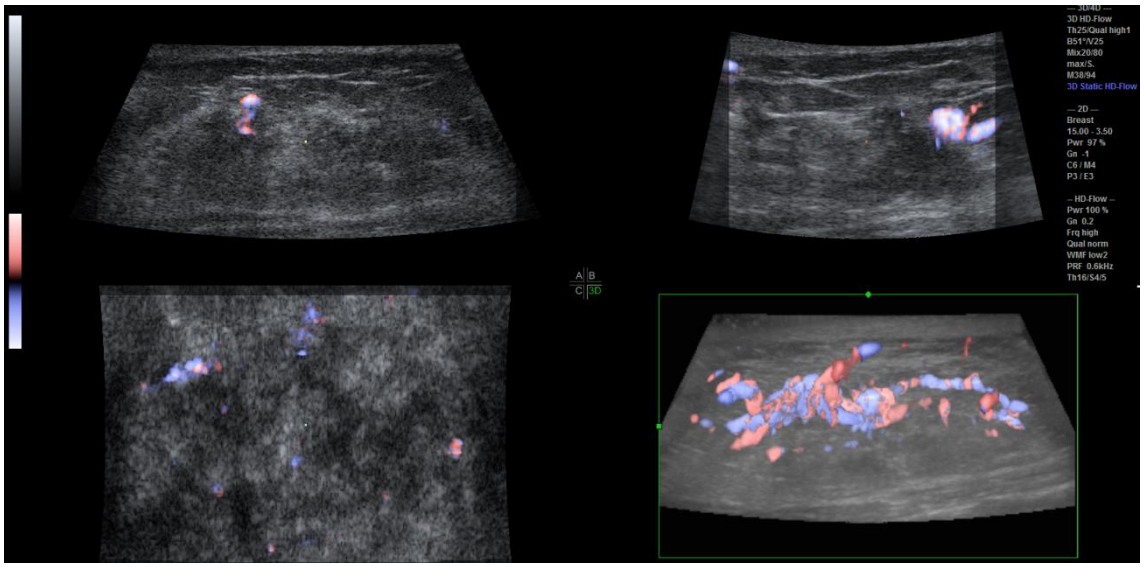

(e)

Figure 2.2: 3D HDF power Doppler ultrasound image of (a) luminal A (b) luminal B1 (c) luminal B2 (d) HER2 overexpressing (e) TN patient from the software GE Kretz 4D View

CHATPER 3

METHODS

3.1 Features Extraction

All the images from 76 patients were obtained by 3D power Doppler ultrasound with HDF function and then transferred to hard disk on personal computer using DICOM (Digital Imaging and Communications in Medicine) format. In this study, all the 3D ultrasonography contained 155 to 199 2D images, and the resolution of each 2D image was approximately 200 × 200 pixels. The partial manual sketching (PMS) system, operated by experienced sonography physicians, is identical to virtual organ computer-aided analysis (VOCAL) scheme within 4D View software and performed to obtain the 3D contour of breast cancer tumor. Figure 3.1 shows that the physician manually sketched six preliminary tumor contours in 0^o, 30^o, 60^o, 90^o, 120^o, and 150^o slice images to define volume of interest (VOI) of tumor. According to those slice images, this study could simulated the 3D model of tumor and displayed the vascular in the tumor.

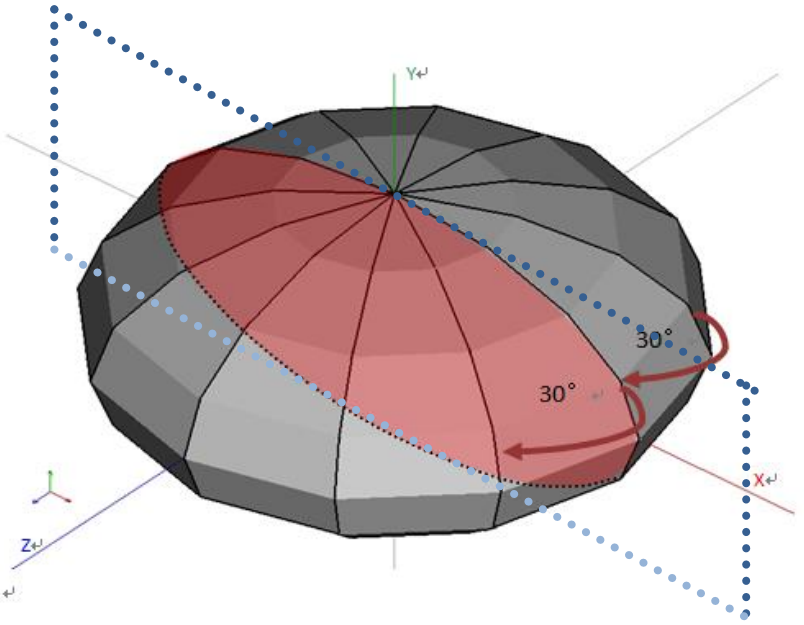

Figure 3.1: The tumor contour that manually sketched with 30^{o} by experienced physician

After VOI extraction, the vascular images were smoothed by the 3D Gaussian low-pass filter [24]. Then the centre-lines of each vessel were be extracted by an automatic extracting method which utilized an efficient parallel 3D 6-subiteration thinning algorithm. The result of vascular centre-lines extraction is showed on Fig. 3.2. This approach appeared excellent because that directly extracted vascular centre-lines from elongated 3D binary objects; accordingly, it provided good results and preserved topology.

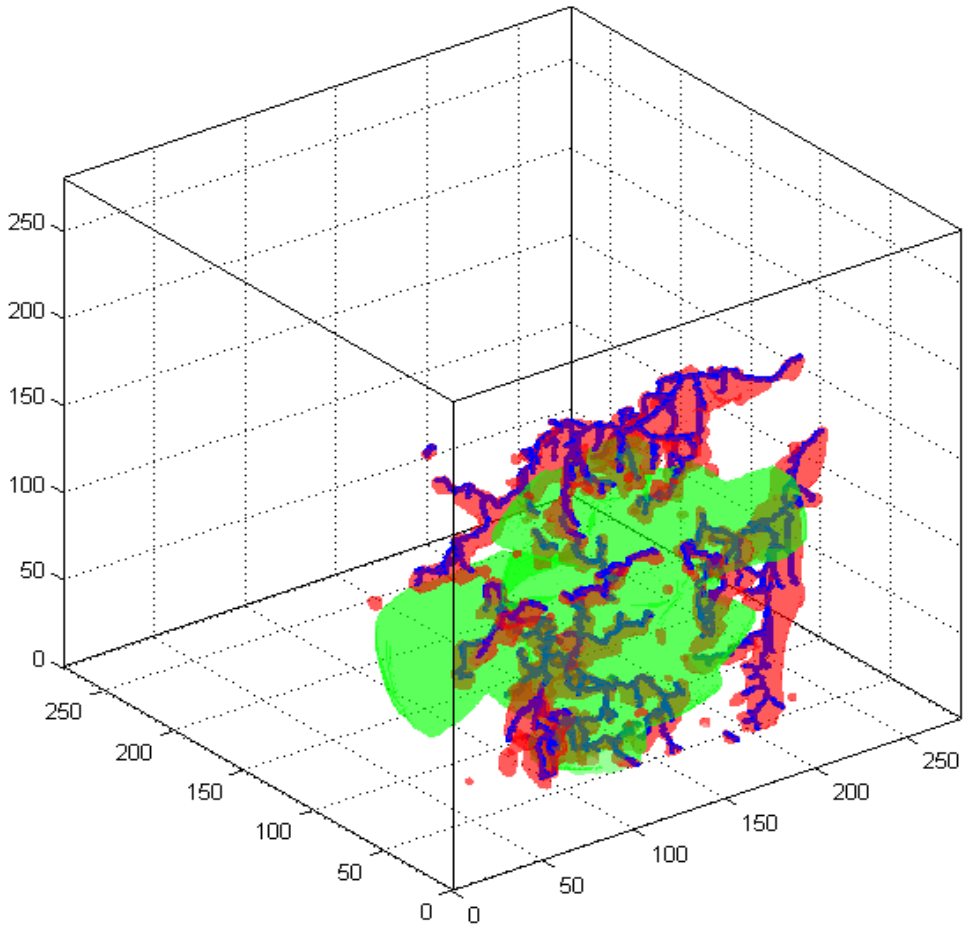

Figure 3.2: The result of vascular centre-lines extraction: the blue lines are the extracted vascular centre-lines, the red regions are blood vessels and the green area is VOI of tumor

3.1.1 Vascular Features

All the flow direction values in the *XY* slice were made from the intensity histogram statistics in the vascular direction channel which ranged within 1 to 255. Notice that the intensity-value 128 is represented the back ground or the direction that perpendicular to the probe. Intensity-values 1 to 127 represented the speed of flow away the probe and intensity-values 129 to 255 represented the speed of flow close to the probe. This study calculated the intensity-value of histogram to extract vascular direction feature.

Let *z* is a random variable indicating intensity, *p(z)* is the histogram of the intensity levels in a specific region. The entropy of vascular direction (denoted *EN*) is a measure of disorder for vascular direction. The *EN* is defined as

$$EN = -\sum_{i=1}^{L} p(z_i)\log_2 p(z_i). \tag{3.1}$$

To quantify the HDF Doppler signal, three indices were evaluated from 3D power Doppler ultrasound. Vascularization index (denoted *VI*), flow index (denoted *FI*) and vascularization flow index (denoted *VFI*) were calculated by values form vessels.

Let S denoted the set of all slices in a 3D power Doppler ultrasound imaging, the *VI* is defined as

$$VI = \frac{\sum_{s\in S} P(s)}{\sum_{s\in S} N(s)}, \tag{3.2}$$

where *P(s)* is the number of voxels with power Doppler signal and *N(s)* is the number of total voxels in the specific area of the slice *s*. *FI* is the mean energy per colour voxel, that represents the average intensity of flow. The *FI* is defined as

$$FI = \frac{\sum_{s\in S} I(s)}{\sum_{s\in S} P(s)}, \tag{3.3}$$

where *I(s)* is the intensity sum of voxels with power Doppler signal in the specific area of the slice *s*. The *VFI* means colour value in all the voxels in the obtained volume, represents both vascularization and flow. The *VFI* for the specific area of the slice s is defined as

$$VFI = \frac{\sum_{s \in S} I(s)}{\sum_{s \in S} N(s)}. \tag{3.4}$$

Except of power Doppler, ultrasound has another type which was color flow mapping (CFM) Doppler. In the CFM histogram, the statistical calculation of the *FI* treats red and blue like one color. In the power Doppler, the histogram has only one color, the *FI* value is the average shade of all orange voxels in the volume. Table 3.1 shows the example that the range of colored signals displayed in the volume. Thus, both *FI* and *CFM_FI* was used in this paper. The definition of *CFM_FI* is same as *FI* but *CFM_FI* is extracted from CFM Doppler ultrasound.

Table 3.1: The range of colored signals displayed in the volume

Power Doppler		Color Flow Mapping (CFM) Doppler	
bright orange	100%	bright red	100%
medium orange	50%	medium red	50%
dark orange	20%	black (middle of color bar)	0%
black	0%	medium blue	50%
		bright blue	100%

3.1.2 Morphological Features

The morphological features were obtained after the constructed vascular trees and the extracted vascular centre-lines. This paper estimated six characteristics including maximum radian between vessels and the tumor center (denoted *MR*), number of branch (denoted *NB*), number of tree (denoted *NT*), number of intree (denoted *NI*), shortest distance between vessels and the tumor center (denoted *SD*) and variance of vessels (denoted *VAR*).

After image pre-processing, the vascularity centre-lines matrix (*Cm*) would be estimated. The *Cm* defined as each point in this matrix stored the result of the 3D images after thinning and multiple voxels wide skeletons (MVWS) elimination in the vascularity centre-lines. The point in *Cm* was assigned to 255 when it belong to centre-lines; otherwise, assigned to 0 when that point not belong to centre-lines. Besides, let *Adj(i)* are the points in the (26, 6)-connectivity of *i*. This study also used pre-processed image matrix (*Im*) that was a result of the 3D images binary converting and noise reduction by morphological operations. Each point in *Im* was assigned by 255 ($\geq T_{voxel}$); otherwise, 0 ($< T_{voxel}$).

All the features in this study are described as follows:

1. *MR*: The average of the radius of vascularity centre-lines in *Cm*.

   To calculate the *MR*, this study applied an iterative loop morphological erosion operator to erode *Im* until no point can be removed. When a point in *Im* was tending to disappear during the iterative loop erosion and there was a point with the same coordinate in *Cm*, then the radius of this point was the execution times of erosion. The *MR* is defined as

$$MR = \frac{\sum_{i \in Cm} MR(i)}{P(Cm)}, \tag{3.5}$$

   where *MR(i)* is the radius of the point *i* in *Cm*.

2. *NB*: The number of branching point of vascularity centre-lines in *Cm*.

   A point had three or more points in the (26, 6)-connectivity of this point was regarded as a branching point. The *NB* is defined as

$$NB = \sum_{i \in Cm} j, \tag{3.6}$$

where $j = 1$ when $|Adj(i)| \geq 3$; otherwise, 0. The value of $|Adj(i)|$ is the total number of the points in $Adj(i)$.

3. *NT*: The number of vascularity centre-lines in *Cm*.

   A connecting region in *Cm* was regarded as vascularity centre-lines. When one or more points of a centre-lines locate were inside of the VOI, this centre-lines was belong to the inside VOI, and so did for boundary VOI.

4. *NI*: The number of vascularity centre-lines in *Cm* but the calculated part only in the tumor.

5. *SD*: The shortest distance between the vascular centre-lines and the barycentre of tumor. The *SD* defined as

$$SD = \min((X_i\text{-}x)^2 + (Y_i\text{-}y)^2 + (Z_i\text{-}z)^2), \tag{3.7}$$

   where (*x, y, z*) was the coordinate of barycentre and $\forall i \in C_{m_i}$ (*Xi*, *Yi*, *Zi*) was the coordinate of point i.

6. *VAR*: The variance of vascularity centre-lines in *Cm*. The *VAR* defined as

$$VAR = \mathrm{E}[(Cm - \mu)^2], \tag{3.8}$$

   where $\mathrm{E}[Cm]$ was the expected value of *Cm*.

3.1.3 Tumor Quantification Features

The tumor quantification features from images usually be used to prognosis the effect of neo-adjuvant. In this paper, we also used basic tumor quantification features that calculated from tumor including tumor volume (denoted *VOL*) and maximum diameter of tumor (denoted *DIA*).

3.2 Statistical Analysis

The neo-adjuvant chemotherapy included six to eight courses. To prognosis the effect of neo-adjuvant chemotherapy in early stage, the first three courses were choose to perform analysis in our study, i.e. N0, N1, N2 and N3 stages. The stage N0 was the sonography before the neo-adjuvant chemotherapy. After every course, patients must take sonographic examination. The stage N1 refers to the first sonographic examination, stage N2 is the second and the third examination is stage N3. In order to compare the differences of each stage, the value of stages were subtracted each other and then established normalization. Therefore, six periods in this study would be obtained as follows:

- N0-N1: difference between stage N0 and stage N1.
- N0-N2: difference between stage N0 and stage N2.
- N0-N3: difference between stage N0 and stage N3.
- N1-N2: difference between stage N1 and stage N2.
- N1-N3: difference between stage N1 and stage N3.
- N2-N3: difference between stage N2 and stage N3.

The 3D HDF Doppler ultrasound imaging of CR, PR, SD and PD cases are showed in Figs. 3.3 to 3.6. Besides, Figs. 3.7 to 3.11 shows the images of molecular subtypes.

Analysis of variance (ANOVA) is a very common model by data analysis that is a method to found association between dependent variable of continuous data type and independent variable of category data type. In statistic, one-way ANOVA is a technique using the F distribution that used to compare means of more than two samples. Actually, ANOVA [25] is a method to present the significance between means of two groups data based on t-test. In this study, all the data were pre-processed by using the Microsoft Excel. Then, the processed data was imported to statistic software Statistical Package for Social Science version 22.0 (SPSS, Inc., Chicago, IL, USA) to executed one-way ANOVA test.

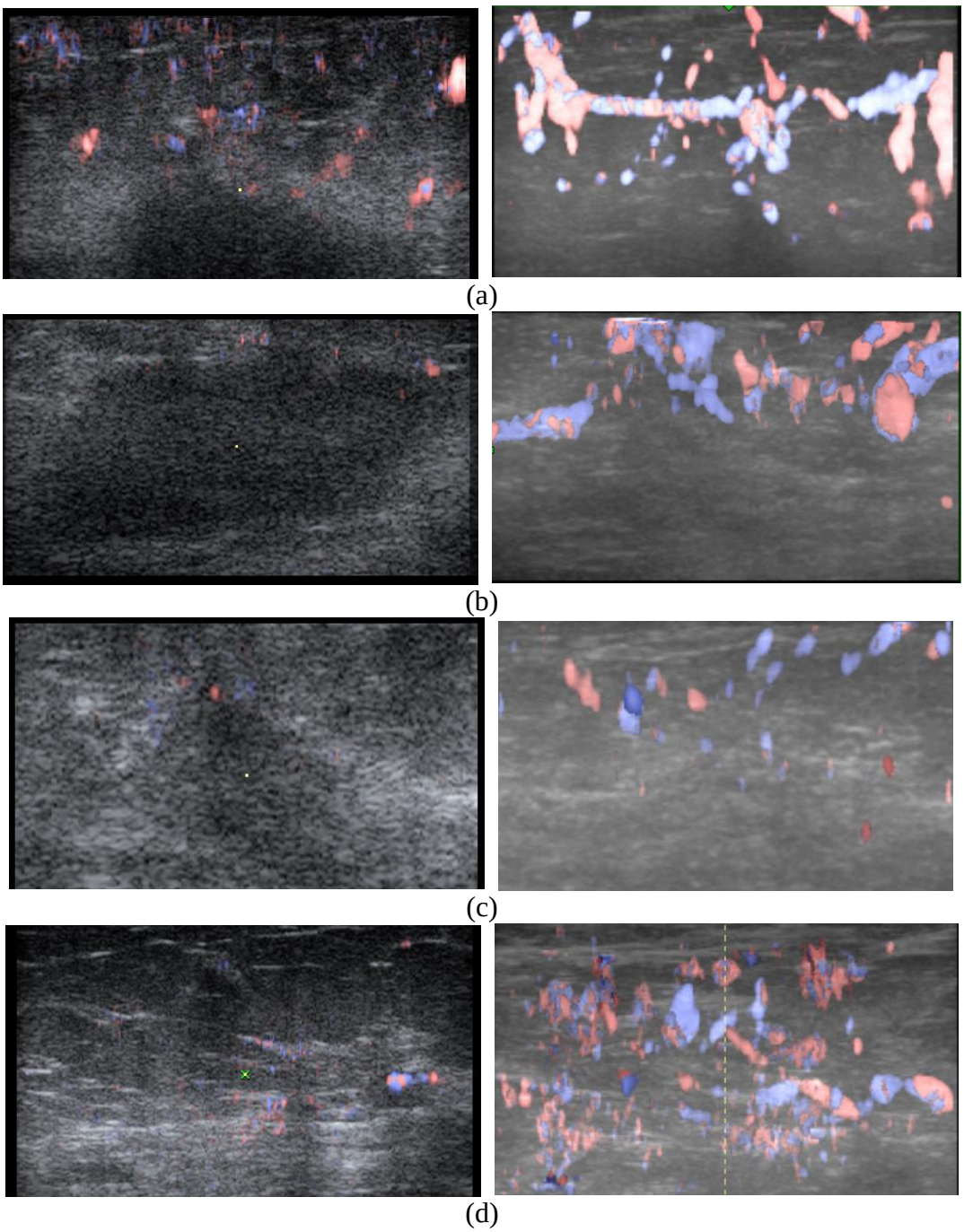

Figure 3.3: The 3D HDF Doppler ultrasound image that vascularity of a CR patient at (a) stage N0, (b) stage N1, (c) stage N2 and (d) stage N3: the left column is 2D image at B-mode and the right column is 3D model of vascularity

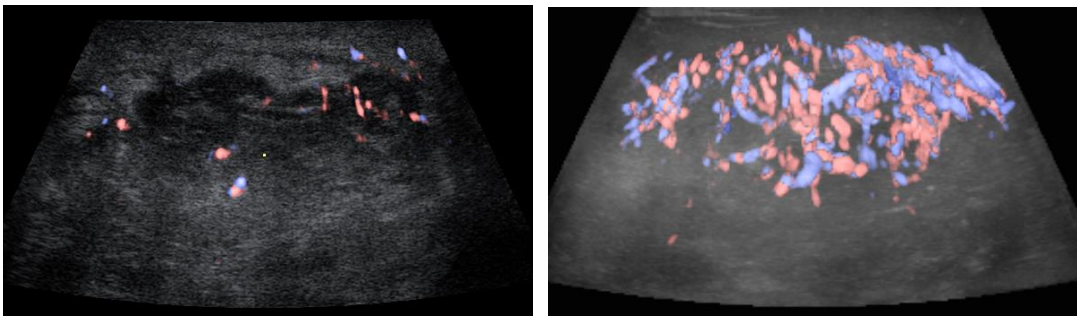

(a)

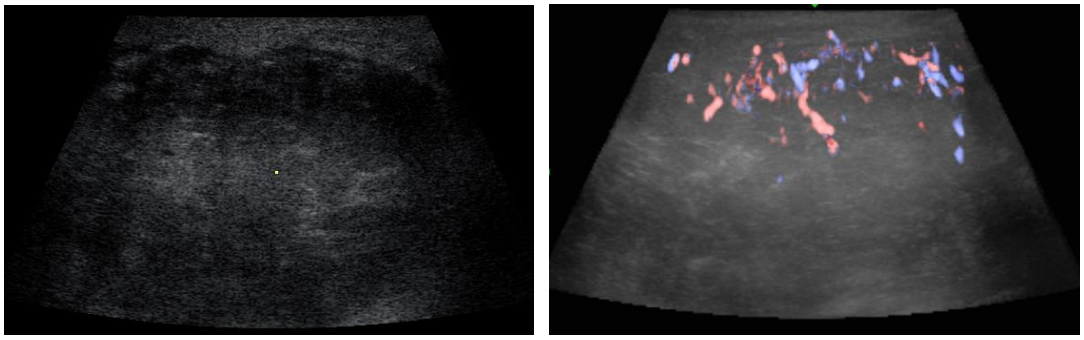

(b)

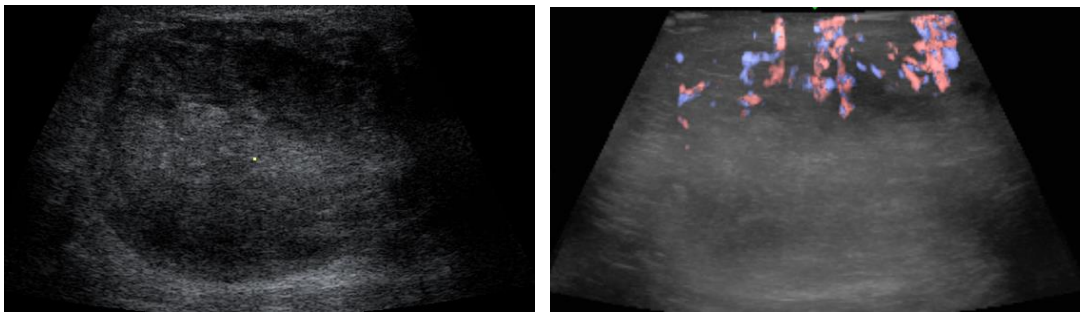

(c)

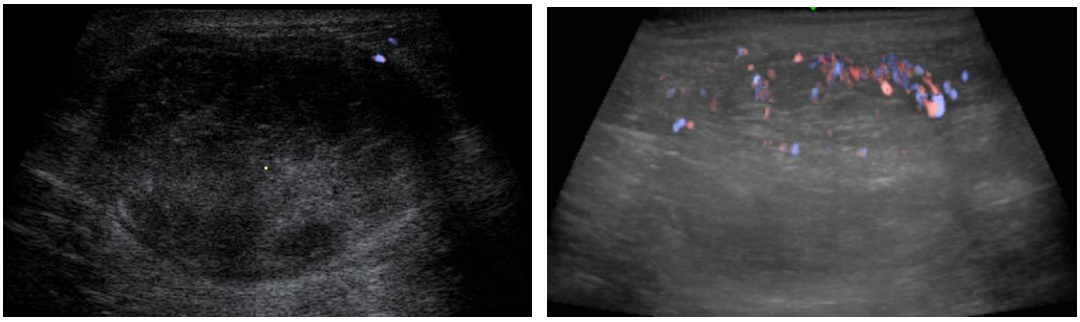

(d)

Figure 3.4: The 3D HDF Doppler ultrasound image that vascularity of a PR patient at (a) stage N0, (b) stage N1, (c) stage N2 and (d) stage N3: the left column is 2D image at B-mode and the right column is 3D model of vascularity

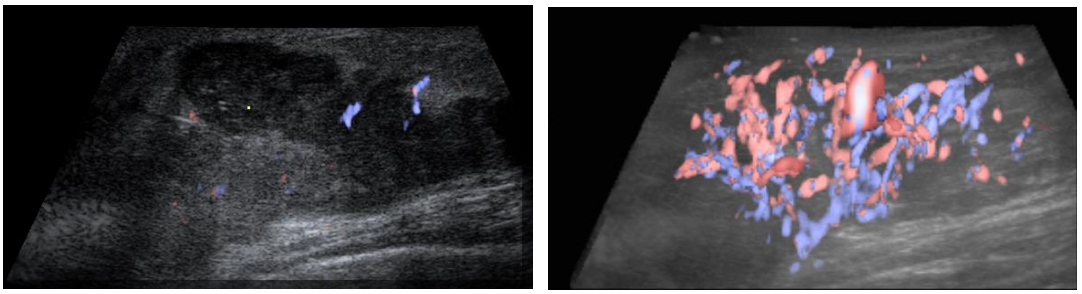

(a)

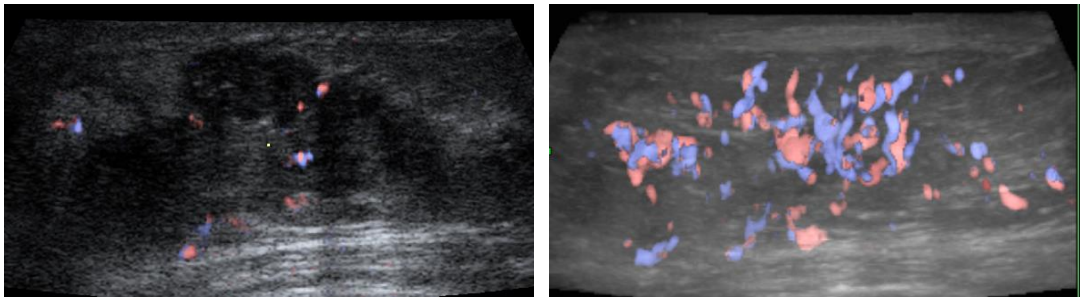

(b)

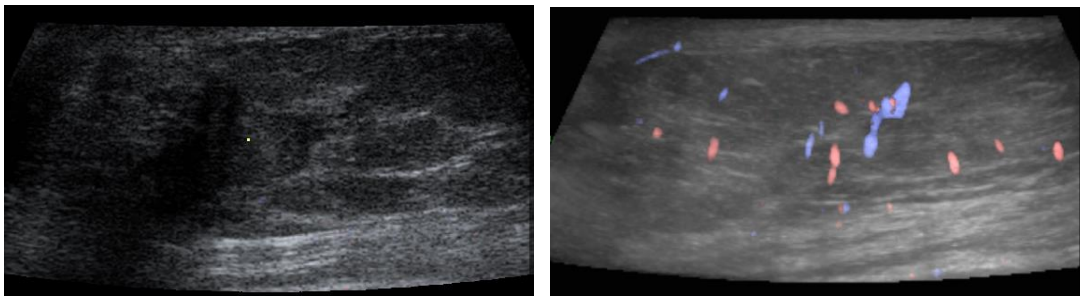

(c)

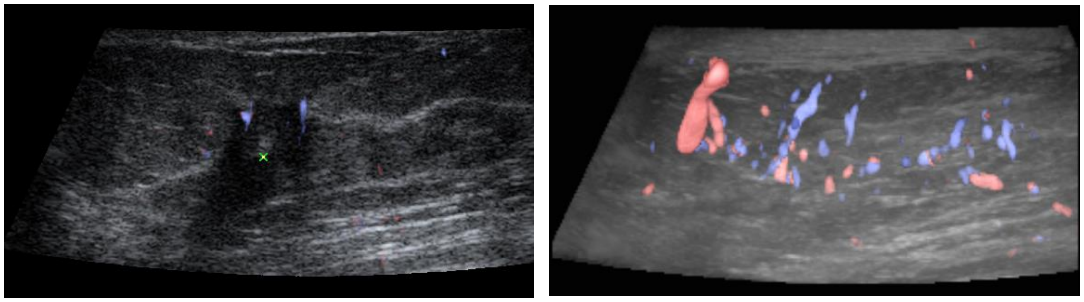

(d)

Figure 3.5: The 3D HDF Doppler ultrasound image that vascularity of a SD patient at (a) stage N0, (b) stage N1, (c) stage N2 and (d) stage N3: the left column is 2D image at B-mode and the right column is 3D model of vascularity

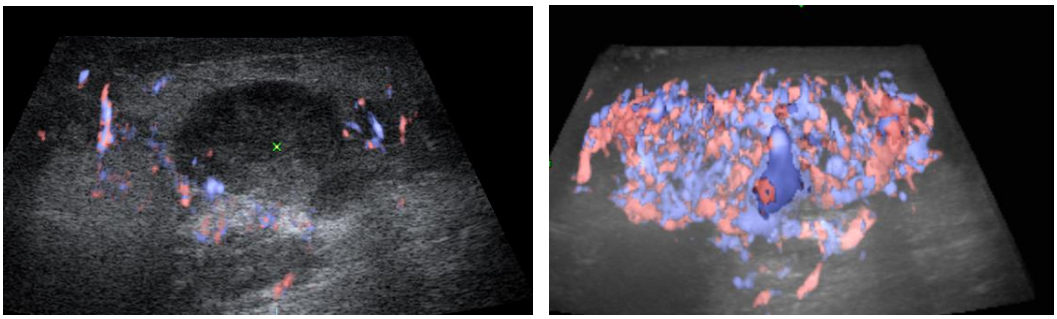

(a)

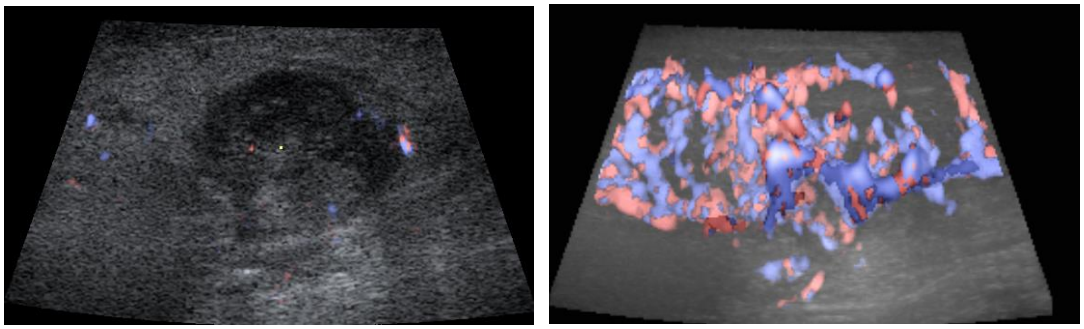

(b)

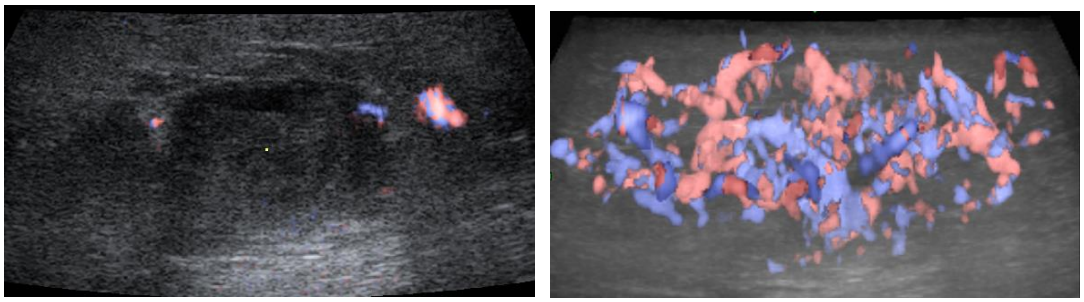

(c)

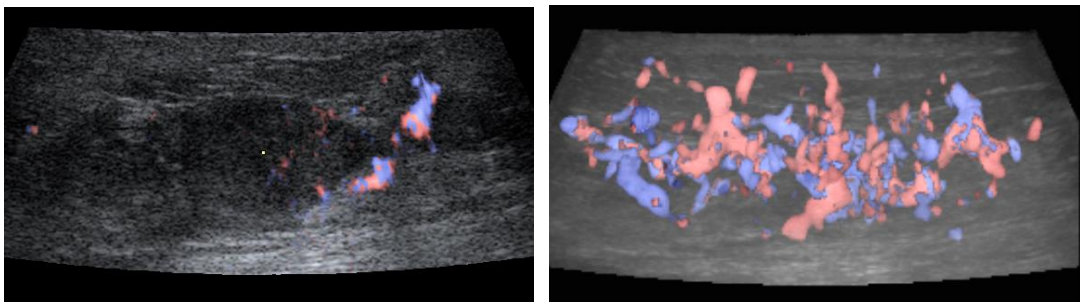

(d)

Figure 3.6: The 3D HDF Doppler ultrasound image that vascularity of a PD patient at (a) stage N0, (b) stage N1, (c) stage N2 and (d) stage N3: the left column is 2D image at B-mode and the right column is 3D model of vascularity

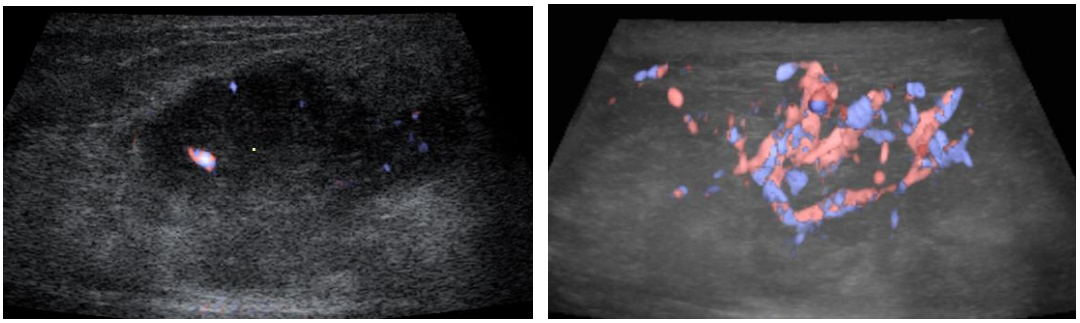

(a)

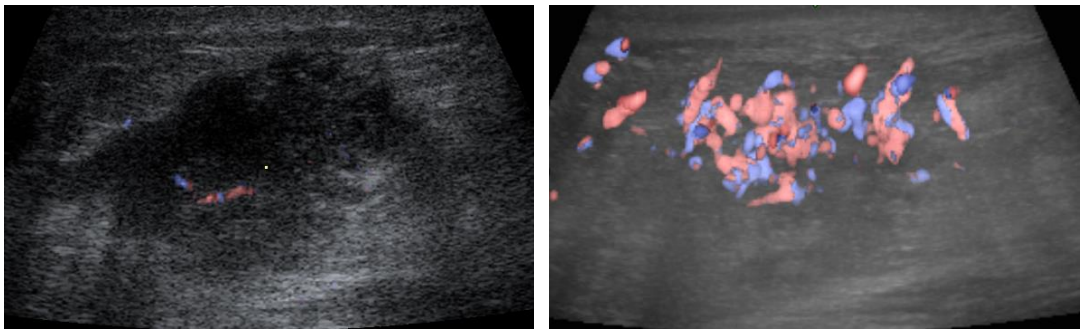

(b)

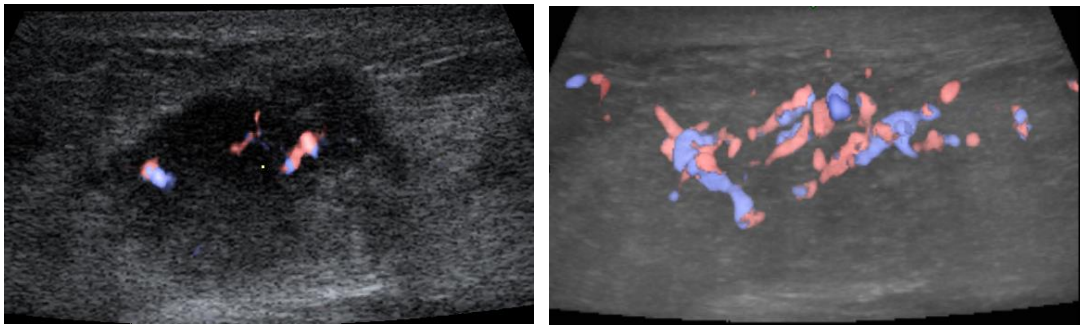

(c)

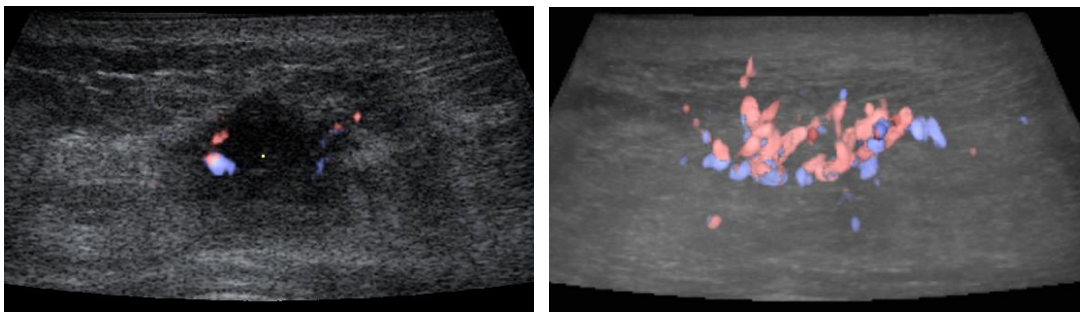

(d)

Figure 3.7: The 3D HDF Doppler ultrasound image that vascularity of a luminal A patient at (a) stage N0, (b) stage N1, (c) stage N2 and (d) stage N3: the left column is 2D image at B-mode and the right column is 3D model of vascularity

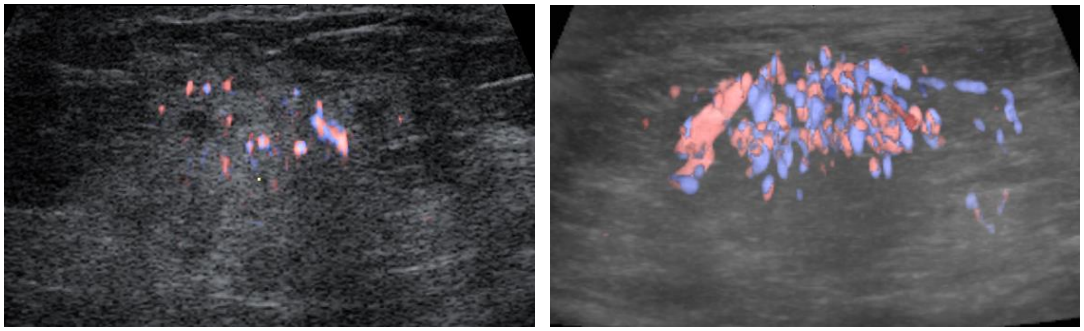

(a)

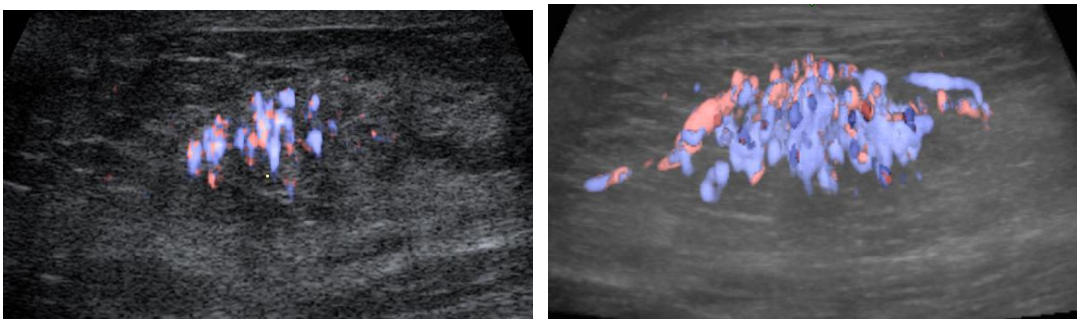

(b)

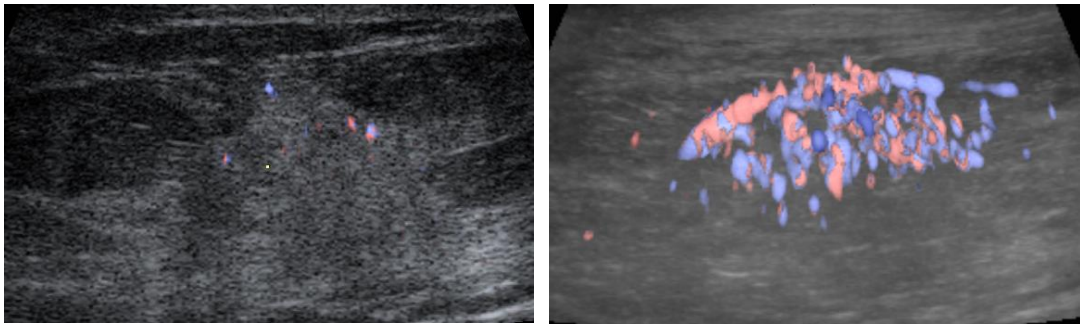

(c)

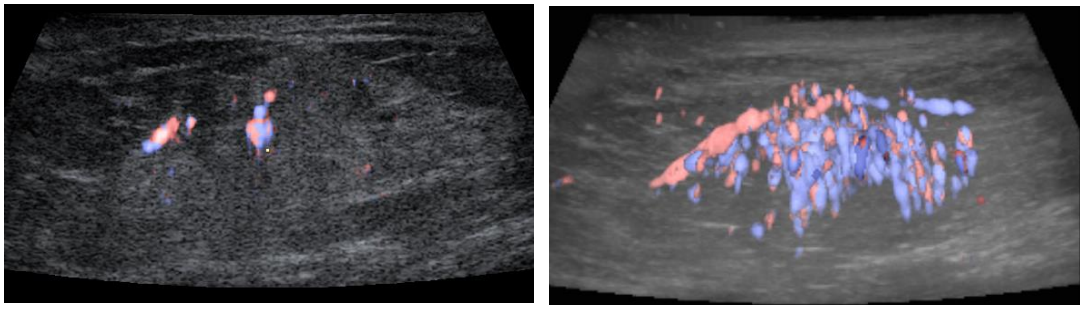

(d)

Figure 3.8: The 3D HDF Doppler ultrasound image that vascularity of a luminal B1 patient at (a) stage N0, (b) stage N1, (c) stage N2 and (d) stage N3: the left column is 2D image at B-mode and the right column is 3D model of vascularity

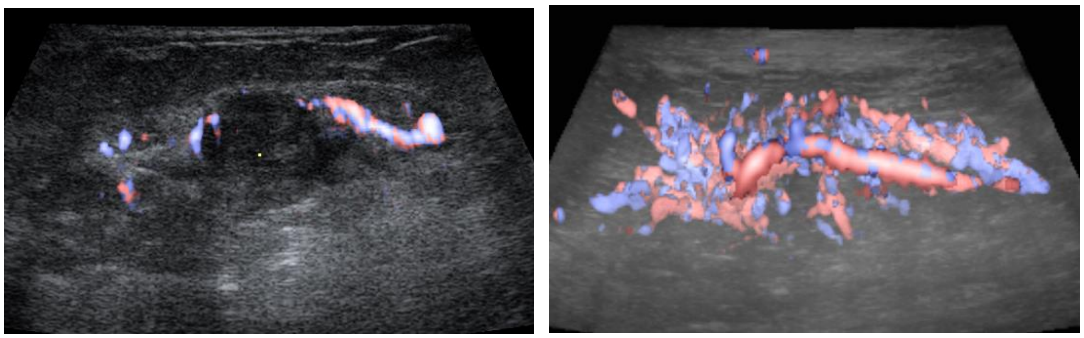

(a)

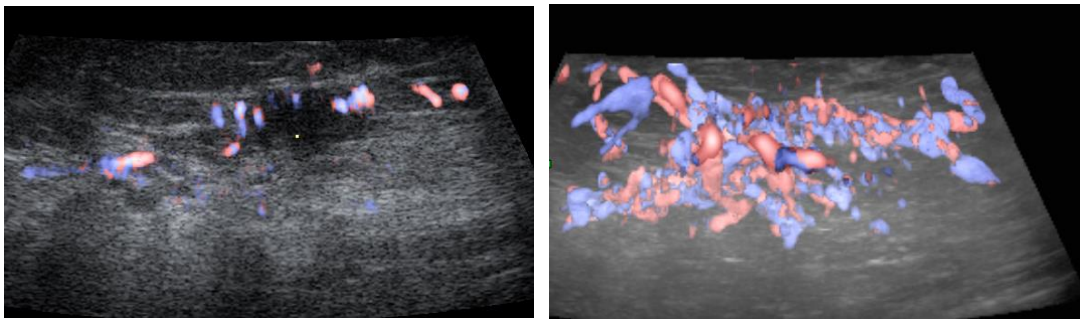

(b)

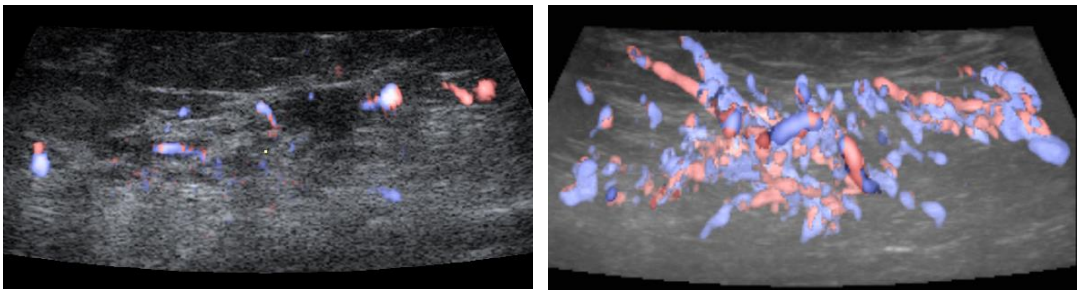

(c)

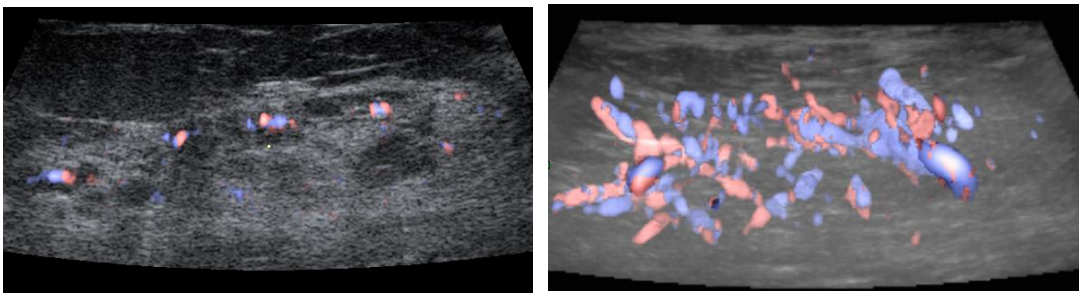

(d)

Figure 3.9: The 3D HDF Doppler ultrasound image that vascularity of a luminal B2 patient at (a) stage N0, (b) stage N1, (c) stage N2 and (d) stage N3: the left column is 2D image at B-mode and the right column is 3D model of vascularity

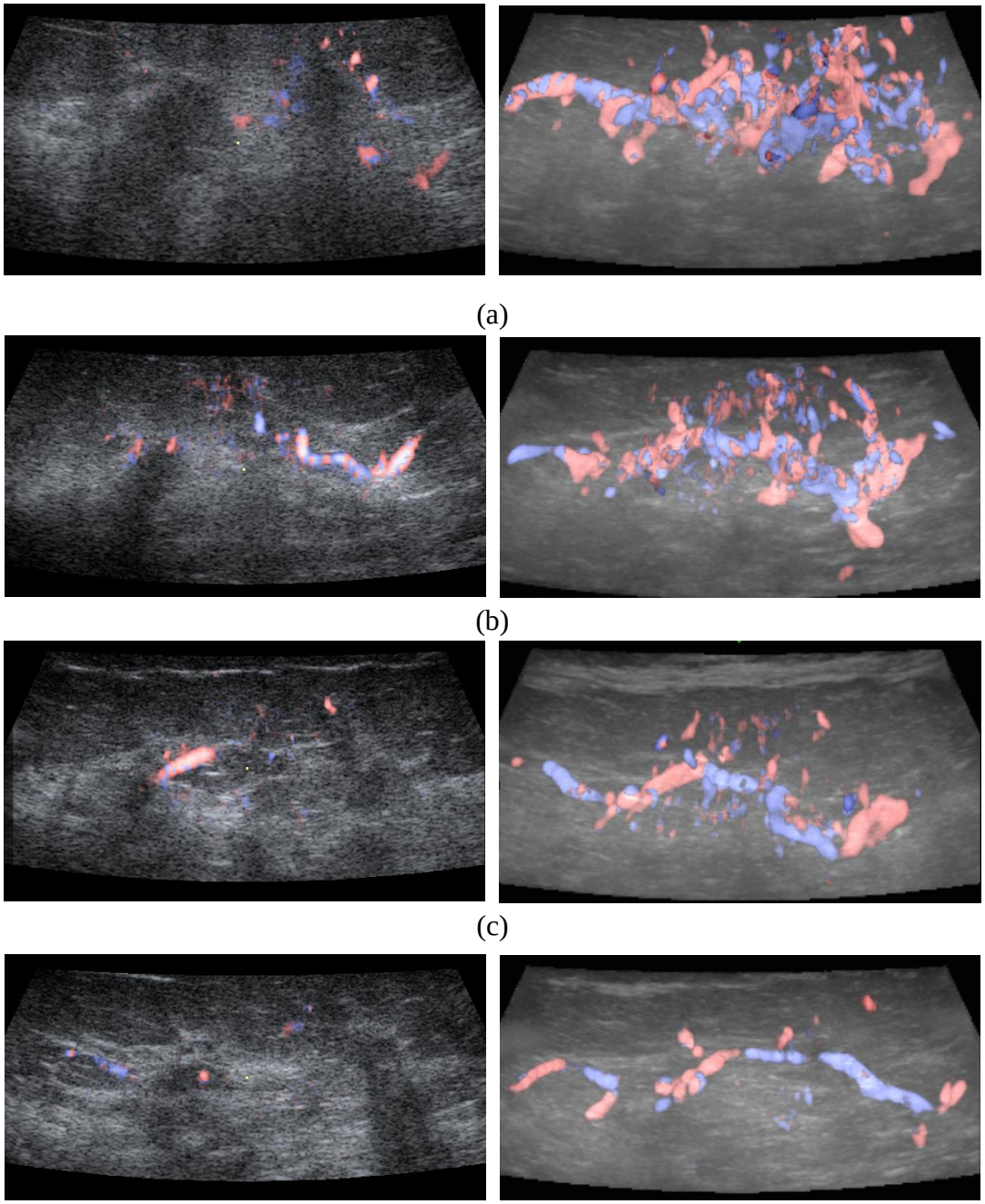

Figure 3.10: The 3D HDF Doppler ultrasound image that vascularity of a HER2 overexpressing patient at (a) stage N0, (b) stage N1, (c) stage N2 and (d) stage N3: the left column is 2D image at B-mode and the right column is 3D model of vascularity

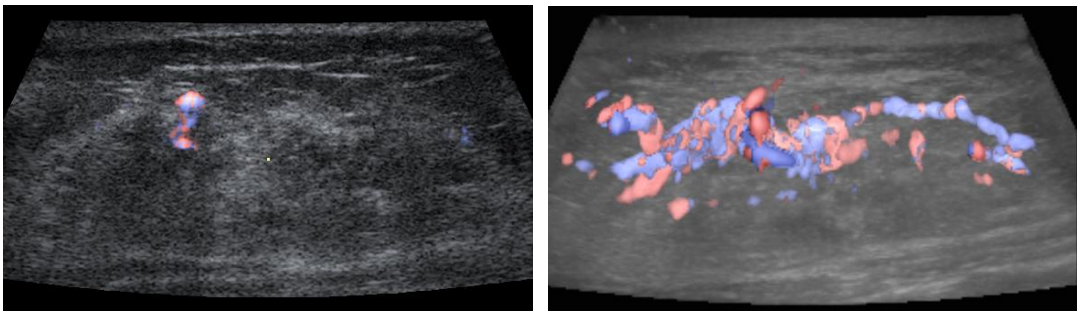

(a)

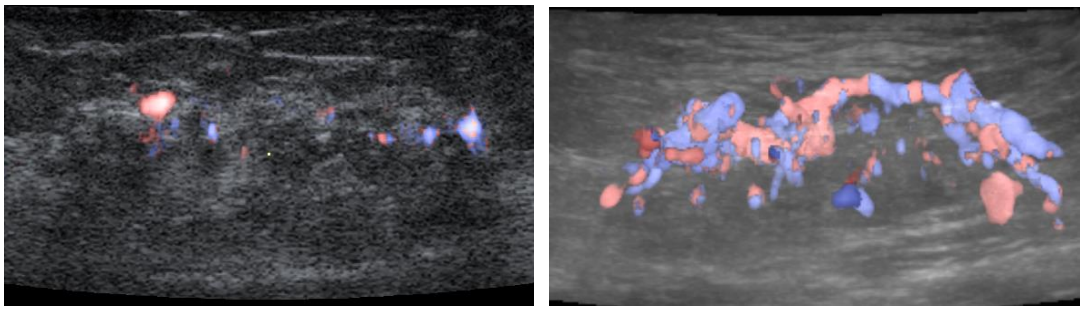

(b)

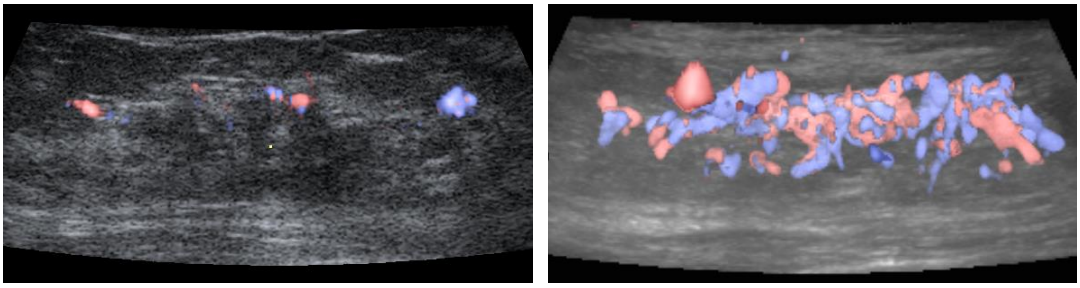

(c)

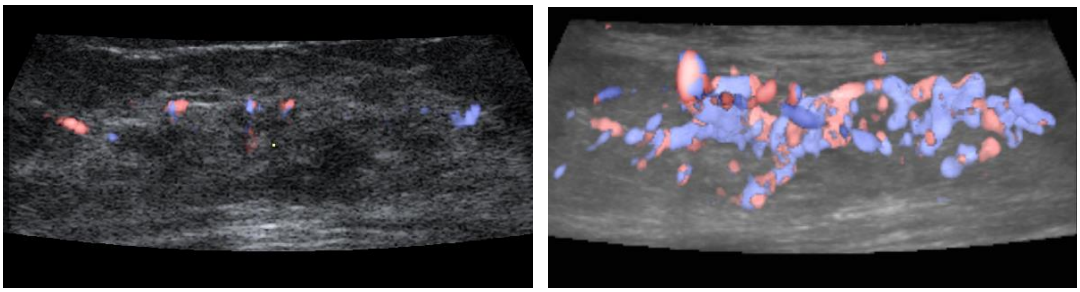

(d)

Figure 3.11: The 3D HDF Doppler ultrasound image that vascularity of a TN patient at (a) stage N0, (b) stage N1, (c) stage N2 and (d) stage N3: the left column is 2D image at B-mode and the right column is 3D model of vascularity

CHAPTER 4

RESULTS

Data set of this study included 76 patients. Every patient contained 13 breast tumor features from the 3D HDF power Doppler ultrasound images at six periods. Tables 4.1 to 4.6 show the means value and standard deviation which presented the distribution of data. The value in the tables was the means value and standard deviation of each features which corresponded to five molecular subtypes.

In six periods, the p-value of each feature is showed in Tables 4.7 to 4.9. The significance of features correspond to every period was presented. Table 4.7 shows the significance of VOL and DIA, the tumor quantification features, in six periods. The p-value of DIA is 0.060 in the period N0-N2 and 0.006 in the period N1-N2. Thus, DIA might associate to stage N2.

Even most p-values of vascular features did not reach statistical significance as shown in Table 4.9, but EN still has significant difference in period N2-N3. The p-value of EN is 0.016. This means that the entropy of vessels might change after stage N2, thus EN could be observed significant difference at period N2-N3.

The p-value of morphological features is also listed in Table 4.8. It is worth mentioning that significance of SD is 0.009 in period N0-N2 and period N1-N2, 0.026 in period N0-N3. According the result, SD might be able to utilize as an effective feature after stage N2.

Table 4.1: Features correspond to molecular subtypes in stage N0-N1.

	Luminal A	Luminal B1	Luminal B2	HER2	TN
VOL	0.054±0.219	-0.188±0.313	-0.295±0.319	-0.297±0.279	-0.369±0.318
DIA	-0.010±0.092	-0.021±0.161	-0.071±0.166	-0.027±0.166	-0.132±0.147
VI	0.284±1.029	0.927±2.127	0.728±3.095	0.949±0.953	2.317±5.745
FI	-0.003±0.152	0.019±0.124	-0.029±0.099	-0.009±0.069	-0.087±0.097
VFI	0.409±1.250	1.094±2.529	0.672±2.834	0.956±0.999	2.423±6.129
CFM_FI	-0.008±0.030	-0.006±0.060	0.003±0.094	0.007±0.051	-0.036±0.047
MR	0.407±0.354	0.079±0.420	0.093±0.426	0.008±0.278	0.103±0.678
NB	1.028±2.305	1.263±7.046	0.007±0.780	0.227±0.704	1.173±3.341
NT	0.341±0.816	0.267±1.166	-0.134±0.452	0.215±0.637	0.140±0.469
NI	0.258±0.477	0.178±0.968	-0.142±0.473	0.154±0.654	0.328±0.489
SD	0.431±1.230	1.846±10.44	1.132±2.481	7.931±16.59	3.415±6.476
VAR	0.019±0.551	0.233±0.828	0.027±0.611	0.194±0.364	0.338±0.977
EN	0.054±0.759	0.682±2.062	0.223±1.213	0.451±0.676	1.286±3.170

TN: triple negative breast cancer;

VOL: volume; *DIA*: diameter; *VI*: vascularization index; *FI*: flow index; *VFI*: vascularization flow index; *MR*: maximum radian between vessels and the tumor center; *NB*: number of branch; *NT*: number of tree; *NI*: number of intree; *SD*: shortest distance between vessels and the tumor center; *VAR*: variance of vessels; *EN*: entropy of vascular direction.

Table 4.2: Features correspond to molecular subtypes in stage N0-N2.

	Luminal A	Luminal B1	Luminal B2	HER2	TN
VOL	-0.290±0.161	-0.395±0.274	-0.521±0.312	-0.412±0.225	-0.462±0.332
DIA	-0.050±0.085	-0.142±0.129	-0.182±0.144	-0.054±0.108	-0.088±0.098
VI	0.001±0.306	0.586±1.658	1.389±4.243	0.533±1.002	0.777±2.249
FI	-0.053±0.080	-0.006±0.171	-0.037±0.168	-0.025±0.117	-0.164±0.152
VFI	-0.046±0.321	0.744±2.215	1.443±4.173	0.545±1.067	0.761±2.282
CFM_FI	-0.022±0.051	0.000±0.095	0.009±0.053	0.003±0.083	-0.065±0.151
MR	-0.018±0.485	-0.096±0.371	-0.028±0.484	-0.075±0.336	-0.267±0.637
NB	0.304±1.241	-0.025±1.245	-0.060±0.886	0.096±0.805	0.309±1.555
NT	0.184±0.469	-0.183±0.703	-0.203±0.586	-0.067±0.695	0.043±1.062
NI	0.286±0.557	-0.012±0.924	-0.347±0.418	0.005±0.809	0.339±1.685
SD	0.116±0.839	2.813±14.58	11.68±39.42	39.46±108.4	478.92±978.4
VAR	-0.077±0.171	0.015±0.797	0.066±0.680	0.112±0.479	-0.007±0.904
EN	-0.138±0.342	0.217±1.291	0.369±1.326	0.256±0.680	0.445±1.610

TN: triple negative breast cancer;

VOL: volume; *DIA*: diameter; *VI*: vascularization index; *FI*: flow index; *VFI*: vascularization flow index; *MR*: maximum radian between vessels and the tumor center; *NB*: number of branch; *NT*: number of tree; *NI*: number of intree; *SD*: shortest distance between vessels and the tumor center; *VAR*: variance of vessels; *EN*: entropy of vascular direction.

Table 4.3: Features correspond to molecular subtypes in stage N0-N3.

	Luminal A	Luminal B1	Luminal B2	HER2	TN
VOL	-0.542±0.082	-0.505±0.261	-0.462±0.465	-0.506±0.156	-0.437±0.415
DIA	-0.149±0.071	-0.147±0.177	-0.159±0.185	-0.054±0.103	-0.151±0.224
VI	1.030±2.030	0.108±0.951	0.622±3.378	0.039±0.738	0.260±1.544
FI	0.005±0.104	-0.058±0.222	-0.074±0.139	-0.032±0.146	-0.164±0.179
VFI	1.212±2.472	0.151±1.088	0.628±3.487	0.050±0.784	0.250±1.544
CFM_FI	-0.036±0.038	-0.017±0.178	0.015±0.072	0.032±0.087	0.006±0.052
MR	0.126±0.446	-0.171±0.364	-0.148±0.456	-0.125±0.364	-0.114±0.571
NB	0.176±0.927	-0.335±0.906	-0.313±0.847	-0.374±0.471	0.060±1.205
NT	0.021±0.259	-0.342±0.507	-0.364±0.526	-0.262±0.496	-0.093±1.102
NI	0.350±0.382	-0.238±0.613	-0.422±0.474	-0.190±0.575	-0.013±1.100
SD	0.095±1.208	1.426±4.536	17.04±58.76	19.27±47.46	64.66±91.41
VAR	0.019±0.307	-0.188±0.548	-0.222±0.611	-0.088±0.406	-0.123±0.657
EN	0.014±0.384	-0.119±0.823	-0.104±0.122	-0.085±0.515	0.055±0.938

TN: triple negative breast cancer;

VOL: volume; *DIA*: diameter; *VI*: vascularization index; *FI*: flow index; *VFI*: vascularization flow index; *MR*: maximum radian between vessels and the tumor center; *NB*: number of branch; *NT*: number of tree; *NI*: number of intree; *SD*: shortest distance between vessels and the tumor center; *VAR*: variance of vessels; *EN*: entropy of vascular direction.

Table 4.4: Features correspond to molecular subtypes in stage N1-N2.

	Luminal A	Luminal B1	Luminal B2	HER2	TN
VOL	-0.322±0.086	-0.258±0.203	-0.300±0.252	-0.132±0.167	-0.180±0.186
DIA	-0.034±0.109	-0.112±0.124	-0.114±0.087	-0.011±0.130	0.078±0.215
VI	0.604±1.593	0.281±1.794	0.443±1.306	-0.166±0.413	-0.165±1.087
FI	-0.039±0.073	-0.024±0.104	-0.010±0.135	-0.014±0.109	-0.087±0.115
VFI	0.644±1.763	0.295±1.849	0.454±1.272	-0.174±0.448	-0.123±1.214
CFM_FI	-0.014±0.033	0.005±0.076	0.020±0.164	-0.005±0.057	-0.034±0.134
MR	-0.286±0.287	-0.165±0.269	-0.133±0.367	-0.090±0.260	-0.433±0.512
NB	-0.221±0.157	-0.251±0.711	0.534±3.066	-0.070±0.445	-0.258±1.090
NT	-0.002±0.302	-0.288±0.467	0.147±1.715	-0.207±0.384	-0.126±0.712
NI	-0.044±0.151	-0.183±0.624	-0.252±0.288	0.071±0.746	-0.134±0.962
SD	0.051±0.459	4.802±17.24	3.105±7.232	1.065±2.150	36.34±54.83
VAR	0.589±1.687	0.059±1.656	0.209±1.283	-0.074±0.280	-0.364±0.547
EN	0.705±0.705	0.315±3.272	0.250±1.177	-0.089±0.423	-0.331±0.797

TN: triple negative breast cancer;

VOL: volume; *DIA*: diameter; *VI*: vascularization index; *FI*: flow index; *VFI*: vascularization flow index; *MR*: maximum radian between vessels and the tumor center; *NB*: number of branch; *NT*: number of tree; *NI*: number of intree; *SD*: shortest distance between vessels and the tumor center; *VAR*: variance of vessels; *EN*: entropy of vascular direction.

Table 4.5: Features correspond to molecular subtypes in stage N1-N3.

	Luminal A	Luminal B1	Luminal B2	HER2	TN
VOL	-0.557±0.063	-0.383±0.277	-0.239±0.465	-0.226±0.251	-0.221±0.308
DIA	-0.136±0.082	-0.124±0.151	-0.088±0.150	-0.009±0.153	-0.032±0.170
VI	1.686±2.950	0.178±2.288	0.046±1.010	-0.362±0.475	-0.425±0.642
FI	0.021±0.115	-0.071±0.216	-0.045±0.125	-0.022±0.133	-0.089±0.150
VFI	2.038±3.698	0.254±2.749	0.027±0.952	-0.370±0.439	-0.387±0.715
CFM_FI	-0.029±0.017	-0.011±0.184	0.019±0.102	0.024±0.067	0.044±0.021
MR	-0.196±0.220	-0.236±0.241	-0.197±0.447	-0.103±0.348	-0.233±0.471
NB	0.052±1.111	-0.403±0.567	-0.423±0.439	-0.356±0.490	-0.390±0.665
NT	0.125±0.887	-0.351±0.454	-0.352±0.390	-0.312±0.324	-0.263±0.611
NI	0.185±0.869	-0.338±0.525	-0.400±0.336	0.117±1.325	-0.374±0.593
SD	-0.336±0.244	3.793±8.000	5.046±8.627	0.824±1.051	13.96±26.16
VAR	0.904±2.376	0.079±2.233	-0.302±0.359	-0.217±0.295	-0.395±0.435
EN	1.489±3.635	0.522±5.088	-0.362±0.392	-0.272±0.441	-0.438±0.499

TN: triple negative breast cancer;

VOL: volume; *DIA*: diameter; *VI*: vascularization index; *FI*: flow index; *VFI*: vascularization flow index; *MR*: maximum radian between vessels and the tumor center; *NB*: number of branch; *NT*: number of tree; *NI*: number of intree; *SD*: shortest distance between vessels and the tumor center; *VAR*: variance of vessels; *EN*: entropy of vascular direction.

Table 4.6: Features correspond to molecular subtypes in stage N2-N3.

	Luminal A	Luminal B1	Luminal B2	HER2	TN
VOL	-0.347±0.052	-0.137±0.469	0.070±0.378	-0.112±0.202	-0.081±0.294
DIA	-0.102±0.044	-0.005±0.160	0.031±0.141	0.007±0.117	-0.073±0.213
VI	0.879±1.563	0.329±2.231	-0.005±1.430	-0.215±0.493	-0.250±0.306
FI	0.061±0.064	-0.044±0.218	-0.028±0.119	-0.003±0.134	-0.005±0.086
VFI	1.054±1.789	0.390±2.401	0.086±1.903	-0.229±0.464	-0.232±0.360
CFM_FI	-0.014±0.041	-0.010±0.202	0.009±0.108	0.030±0.051	0.107±0.193
MR	0.222±0.369	-0.081±0.278	-0.171±0.262	-0.002±0.317	0.042±0.093
NB	0.205±1.038	0.166±1.823	-0.271±0.404	-0.242±0.482	0.027±0.313
NT	0.110±0.855	0.174±1.390	-0.107±0.501	-0.064±0.465	-0.081±0.270
NI	0.201±0.844	0.294±1.981	-0.087±0.564	-0.051±0.343	-0.083±0.372
SD	-0.229±0.410	3.672±8.919	6.085±13.111	0.425±1.403	0.709±1.629
VAR	0.112±0.310	0.091±0.921	-0.192±0.549	-0.118±0.349	-0.137±0.454
EN	0.262±0.546	0.265±1.605	-0.282±0.616	-0.157±0.482	-0.082±0.653

TN: triple negative breast cancer;

VOL: volume; *DIA*: diameter; *VI*: vascularization index; *FI*: flow index; *VFI*: vascularization flow index; *MR*: maximum radian between vessels and the tumor center; *NB*: number of branch; *NT*: number of tree; *NI*: number of intree; *SD*: shortest distance between vessels and the tumor center; *VAR*: variance of vessels; *EN*: entropy of vascular direction.

Table 4.7: P-value of tumor quantification features for molecular subtypes

	N0N1/N0	N0N2/N0	N0N3/N0	N1N2/N1	N1N3/N1	N2N3/N2
VOL	0.110	0.427	0.970	0.247	0.168	0.225
DIA	0.512	0.060	0.609	0.006	0.221	0.346

VOL: volume; *DIA*: diameter.

Table 4.8: P-value of morphological features for molecular subtypes

	N0N1/N0	N0N2/N0	N0N3/N0	N1N2/N1	N1N3/N1	N2N3/N2
MR	0.498	0.834	0.641	0.269	0.877	0.055
NB	0.927	0.929	0.629	0.578	0.562	0.790
NT	0.643	0.748	0.568	0.626	0.314	0.894
NI	0.603	0.430	0.136	0.723	0.184	0.889
SD	0.444	0.009	0.026	0.009	0.121	0.406
VAR	0.833	0.988	0.891	0.811	0.619	0.684

MR: maximum radian between vessels and the tumor center; *NB*: number of branch; *NT*: number of tree; *NI*: number of intree; *SD*: shortest distance between vessels and the tumor center; *VAR*: variance of vessels.

Table 4.9: P-value of vascular features for molecular subtypes

	N0N1/N0	N0N2/N0	N0N3/N0	N1N2/N1	N1N3/N1	N2N3/N2
VI	0.752	0.761	0.776	0.779	0.287	0.720
FI	0.275	0.295	0.597	0.703	0.748	0.726
VFI	0.756	0.798	0.766	0.789	0.302	0.717
CFM_FI	0.774	0.497	0.794	0.844	0.815	0.586
EN	0.716	0.924	0.990	0.947	0.794	0.016

VI: vascularization index; *FI*: flow index; *VFI*: vascularization flow index; *EN*: entropy of vascular direction.

CHAPTER 5

DISCUSSION AND CONCLUSION

In this decades, pre-diagnosis of breast cancer gradually becomes a more importantly issue. The aim of this study is attempt to find the connection of molecular subtypes. The evaluation results present that the significance of SD might provide special estimation performance at stage N2. Significance of SD is 0.009 in period N0-N2 and period N1-N2, 0.026 in period N0-N3. It means that the treatment of neo-adjuvant chemotherapy might produce changes at stage N2. Also, EN has significant difference in period N2-N3, the p-value of EN is 0.016. In addition, there was presumed that blood vessels of tumor would make a difference at stage N2. The shortest distance of blood vessels would obtain different changes in each subtype at stage N2, and then the entropy of vascular direction would be difference at stage N3.

In otherwise, significant difference in DIA is revealed at stage N2. The tumor quantification features related to each other is means that the volume of tumor would have connection of tumors diameter [26]. However, those tumor quantification features are related by the direction of imaging and that would influence the measuring of diameter and volume [27]. Even the p-value is 0.06 at period N0-N2 and 0.006 at period N1-N2, we still could not heroic assumptions significant difference in DIA is meaningful. The same, we could not deny the relevance of tumor size. There was some papers appeared that the significance of tumor size in predict effect of chemotherapy or classification of breast cancer [28].

Even though this study observed several significant differences, there are many issue of discussion. Our material was estimated to take statistical analysis. Among 76 patients, the case number of neo-adjuvant chemotherapy response was prorated uneven. The case number of some subtypes was no existing even though we have not

complicated classification of breast cancer neo-adjuvant chemotherapy. For example, there were only five cases in PD, but 36 cases in PR. Besides, because case number of PD was minor, there was no patient was belong to luminal B2 and HER2 overexpressing subtypes. Many studies will used the public database like the surveillance, epidemiology, and end results (SEER) datasets, which a premier source for cancer statistics in the United States [29-32]. In order to the result could approach the real situation, the clinical cases are relatively better objects to take statistical analysis.

The most important aim of our study is early predicting the effect of neo-adjuvant chemotherapy [33]. From the results, the significant difference could be observed at stage N2. However, significant difference at stage N1 is more valuable for early predicting. In the future work, there might found more new features of tumor imaging to achieve the aim of early predicting.

REFERENCES

[1] I. Schreer and LC, "Breast cancer: early detection," in *Radiologic-Pathologic Correlations from Head to Toe*, ed: Springer, 2005, pp. 767-784.

[2] A. M. Leitch, G. D. Dodd, M. Costanza, M. Linver, P. Pressman, L. McGinnis, *et al.*, "American Cancer Society guidelines for the early detection of breast cancer: update 1997," *CA: A cancer Journal for Clinicians*, vol. 47, pp. 150-153, 1997.

[3] M. S. O'Malley and S. W. Fletcher, "Screening for breast cancer with breast self-examination: A critical review," *JAMA*, vol. 257, pp. 2196-2203, 1987.

[4] U. Veronesi, G. Paganelli, V. Galimberti, G. Viale, S. Zurrida, M. Bedoni, *et al.*, "Sentinel-node biopsy to avoid axillary dissection in breast cancer with clinically negative lymph-nodes," *The Lancet*, vol. 349, pp. 1864-1867, 1997.

[5] J. G. Elmore, K. Armstrong, C. D. Lehman, and S. W. Fletcher, "Screening for breast cancer," *Jama*, vol. 293, pp. 1245-1256, 2005.

[6] L. NystrC6m, S. Wall, L. Rutqvist, A. Lindgren, M. Lindqvist, S. Ryden, *et al.*, "Breast cancer screening with mammography: overview of Swedish randomised trials," *The Lancet*, vol. 341, pp. 973-978, 1993.

[7] H.-D. Cheng, X. Cai, X. Chen, L. Hu, and X. Lou, "Computer-aided detection and classification of microcalcifications in mammograms: a survey," *Pattern recognition*, vol. 36, pp. 2967-2991, 2003.

[8] S. S. Buchbinder, I. S. Leichter, R. B. Lederman, B. Novak, P. N. Bamberger, H. Coopersmith, *et al.*, "Can the size of microcalcifications predict malignancy of clusters at mammography?," *Academic radiology*, vol. 9, pp. 18-25, 2002.

[9] J. Stone, J. Ding, R. Warren, S. W. Duffy, and J. L. Hopper, "Using mammographic density to predict breast cancer risk: dense area or percentage dense area," *Breast Cancer Res*, vol. 12, p. R97, 2010.

[10] S. Jose, "Texture Feature Extraction for Mammogram Images Using Biorthogonal Wavelet Filter via Lifting Scheme," *International Journal of Science and Research,* vol. 3, pp. 1252-1256, 2014.

[11] T. T. Alagaratnam and J. Wong, "Limitations of mammography in Chinese females," *Clinical radiology,* vol. 36, pp. 175-177, 1985.

[12] R. M. Mann, C. K. Kuhl, K. Kinkel, and C. Boetes, "Breast MRI: guidelines from the European society of breast imaging," *European radiology,* vol. 18, pp. 1307-1318, 2008.

[13] G. I. Whitman, C.-I. Lai, X. Liu, M. Itani, R. Khisty, and C. C. Shaw, "Breast computed tomography," *Digital Mammography: A Practical Approach,* p. 125, 2012.

[14] C. K. Kuhl, S. Schrading, C. C. Leutner, N. Morakkabati-Spitz, E. Wardelmann, R. Fimmers, *et al.,* "Mammography, breast ultrasound, and magnetic resonance imaging for surveillance of women at high familial risk for breast cancer," *Journal of clinical oncology,* vol. 23, pp. 8469-8476, 2005.

[15] D. D. Adler, P. L. Carson, J. M. Rubin, and D. Quinn-Reid, "Doppler ultrasound color flow imaging in the study of breast cancer: preliminary findings," *Ultrasound in medicine & biology,* vol. 16, pp. 553-559, 1990.

[16] L. Hatle and B. Angelsen, *Doppler ultrasound in cardiology: physical principles and clinical applications*: Lea & Febiger, 1985.

[17] C. Nosarti, J. V. Roberts, T. Crayford, K. McKenzie, and A. S. David, "Early psychological adjustment in breast cancer patients: a prospective study," *Journal of Psychosomatic Research,* vol. 53, pp. 1123-1130, 2002.

[18] M. J. Piccart-Gebhart, M. Procter, B. Leyland-Jones, A. Goldhirsch, M. Untch, I. Smith, *et al.,* "Trastuzumab after adjuvant chemotherapy in HER2-positive

breast cancer," *New England Journal of Medicine,* vol. 353, pp. 1659-1672, 2005.

[19] R. Rouzier, C. M. Perou, W. F. Symmans, N. Ibrahim, M. Cristofanilli, K. Anderson, *et al.*, "Breast cancer molecular subtypes respond differently to preoperative chemotherapy," *Clinical Cancer Research,* vol. 11, pp. 5678-5685, 2005.

[20] S. H. Kim, J. M. Lee, Y. J. Kim, J. Y. Lee, J. K. Han, and B. I. Choi, "High-Definition Flow Doppler Ultrasonographic Technique to Assess Hepatic Vasculature Compared With Color or Power Doppler Ultrasonography Preliminary Experience," *Journal of Ultrasound in Medicine,* vol. 27, pp. 1491-1501, 2008.

[21] B. G. Tabachnick, L. S. Fidell, and S. J. Osterlind, "Using multivariate statistics," 2001.

[22] I. F. Faneyte, J. G. Schrama, J. L. Peterse, P. L. Remijnse, S. Rodenhuis, and M. Van de Vijver, "Breast cancer response to neoadjuvant chemotherapy: predictive markers and relation with outcome," *British journal of Cancer,* vol. 88, pp. 406-412, 2003.

[23] D. Allred, J. M. Harvey, M. Berardo, and G. M. Clark, "Prognostic and predictive factors in breast cancer by immunohistochemical analysis," *Modern pathology: an official journal of the United States and Canadian Academy of Pathology, Inc,* vol. 11, pp. 155-168, 1998.

[24] J. Chen, S. Paris, and F. d. Durand, "Real-time edge-aware image processing with the bilateral grid," in *ACM Transactions on Graphics (TOG),* 2007, p. 103.

[25] R. Gueorguieva and J. H. Krystal, "Move over anova: Progress in analyzing repeated-measures data andits reflection in papers published in the archives of general psychiatry," *Archives of general psychiatry,* vol. 61, pp. 310-317, 2004.

[26] R. Kayar, S. Civelek, M. Cobanoglu, O. Gungor, H. Catal, and M. Emiroglu, "Five methods of breast volume measurement: a comparative study of measurements of specimen volume in 30 mastectomy cases," *Breast cancer: basic and clinical research*, vol. 5, p. 43, 2011.

[27] S. C. Partridge, J. E. Gibbs, Y. Lu, L. J. Esserman, D. Tripathy, D. S. Wolverton, *et al.*, "MRI measurements of breast tumor volume predict response to neoadjuvant chemotherapy and recurrence-free survival," *American Journal of Roentgenology*, vol. 184, pp. 1774-1781, 2005.

[28] I. V. Gruber, M. Rueckert, K. O. Kagan, A. Staebler, K. C. Siegmann, A. Hartkopf, *et al.*, "Measurement of tumour size with mammography, sonography and magnetic resonance imaging as compared to histological tumour size in primary breast cancer," *BMC cancer*, vol. 13, p. 328, 2013.

[29] A. M. Schwartz, D. E. Henson, D. Chen, and S. Rajamarthandan, "Histologic grade remains a prognostic factor for breast cancer regardless of the number of positive lymph nodes and tumor size: a study of 161 708 cases of breast cancer from the SEER program," *Archives of Pathology and Laboratory Medicine*, vol. 138, pp. 1048-1052, 2014.

[30] R. Rengan, K. Baker, L. Salazar, J. Childs, D. Higgins, M. Redman, *et al.*, "Abstract P2-11-05: Overall survival in inflammatory breast cancer patients receiving Her-2 Neu directed tumor vaccine therapy: Matched comparison with SEER registry patients," *Cancer Research*, vol. 76, pp. P2-11-05-P2-11-05, 2016.

[31] J. L. Warren, C. N. Klabunde, D. Schrag, P. B. Bach, and G. F. Riley, "Overview of the SEER-Medicare data: content, research applications, and generalizability to the United States elderly population," *Medical care*, vol. 40, pp. IV-3-IV-18, 2002.

[32] D. Delen, G. Walker, and A. Kadam, "Predicting breast cancer survivability: a comparison of three data mining methods," *Artificial intelligence in medicine*, vol. 34, pp. 113-127, 2005.

[33] D. Manton, A. Chaturvedi, A. Hubbard, M. Lind, M. Lowry, A. Maraveyas, *et al.*, "Neoadjuvant chemotherapy in breast cancer: early response prediction with quantitative MR imaging and spectroscopy," *British journal of cancer*, vol. 94, pp. 427-435, 2006.